Faults diagnosis via a dynamical sparse recovery method and application to a gearbox system

Syrine Derbel, Florentina Nicolau, Nabih Feki, Jean Pierre Barbot, Mohamed Abbes, Mohamed Haddar

Faults diagnosis via a dynamical sparse recovery method and application to a gearbox system

Syrine Derbel*[,1,2], Florentina Nicolau [1], Nabih Feki[3], Jean Pierre Barbot [1], Mohamed Slim Abbes[2], and Mohamed Haddar[2]

[1]QUARTZ Laboratory, ENSEA, 6 Avenue du Ponceau, 95014 Cergy-Pontoise, France
[2]LA2MP Laboratory, ENIS, 4 Route de la Soukra, 3038 Sfax, Tunisia
[3]Sousse University, ISSATSo, mechanical department, Sousse, Tunisia

Abstract

With the ever increase of the complexity and the importance of industrial systems, diagnosis techniques allowing to detect, locate and identify any abnormalities in the system as early as possible, have attracted a lot of attention over the past years. In this paper, we present a diagnosis method for nonlinear dynamical systems, called sparse recovery diagnosis (SRD), based on a dynamical algorithm that estimates a sparse fault vector from few system measurements. The term sparse means that many faults can be considered but only few of them can occur simultaneously. In order to illustrate the performances of this diagnosis method, we apply it to a gear power transmission. This dynamical system is among the most important mechanical components in industrial systems. The gear power transmission model considered in this paper is composed by a two-stage gear for which we take into account the torsional effect of the gears. Different sensor and mechanical faults perturbing its operating mode will be modeled and detected by the SRD method.

Keywords: Diagnostic, fault detection, sparse recovery diagnosis, gearbox system, gear power transmission, mechanical faults, sensor faults.

1 Introduction

The diagnostic of industrial systems is one of the most important tasks that ensures the continuity of the production, the safety and the economic aspects in the industries. For these reasons, many diagnosis methods enabling early fault detection have been developed in the literature (see for example, the following surveys [27], [17]). The presence of faults is very often the cause of system performances degradation, and even the damage and the collapse of the whole system. An unexpected fault can affect either the sensors leading to measurement errors (in that case, the fault is called a sensor fault) or the components of the system leading to a change of the system properties (in that case, the fault is called an operating fault).

*corresponding author: syrine.derbel@ensea.fr

The faults diagnosis consists in three important steps: fault detection, fault location and fault identification. The first step enables to detect the presence of a malfunction in the system. Fault isolation consists on determining the location of faulty components, while fault identification allows to identify the type, shape and size of the appeared fault. In general, diagnosis methods are based on the concept of redundancy (see , for example, [17], [24]) which can be of two types: hardware or analytical redundancy. The key idea of the hardware redundancy is to compare duplicated measurements using multiple hardware (for instance, sensors) for the same components and input signals. This comparison allows to take the best diagnostic decision by using different methods such as majority voting, limit checking, *etc.* The analytical redundancy uses specific information given by a mathematical model or historic system data, or signals information. It includes the model-based methods, the signals-based methods and the data-driven methods. Model-based methods such as parity space techniques, observers' methods and parameters estimation have been the object of many papers (see, *e.g.,* the surveys, [22], [25], [28]). Signals-based methods are discussed and applied in many works (see, *e.g.,* [30], [2], [31] and [17]). They contain time domain, frequency domain and time-frequency domain methods. Finally, data-driven techniques, including neural networks and fuzzy logic methods, have been the aim of several research works (see, *e.g.,* [13], [17]).

In this paper, we present a diagnosis method (that we will call sparse recovery diagnosis, or simply SRD method) for nonlinear dynamical systems. The SRD method is inspired from sparse recovery methods ([5], [4]) which are well know in the field of signal processing (where they are often applied for medical imaging and image processing, see, *e.g.,* [9], [18]). From a fault detection point of view, other methods based on similar theories (like compressing sensing theory, sparse decomposition and impulse signal recovery) have been already developed in the literature (*e.g.,* [11], [38], [19], [23], [32]). They are based on the extraction of the fault features through a sparse representation in a specific base (like Fourier, wavelet or cepstral transforms, *etc*, for a spectral representation). In many works on fault diagnosis via sparse recovery techniques, fault characteristics are directly extracted from a small number of random projections without reconstructing the vibration signal completely and with prior fault characteristic frequency knowledge required. On the contrary, the SRD method presented in this paper is based on an analytical system modeling and allows to detect, locate and identify different types of faults affecting the dynamical system. The analytic model contains the healthy and the faulty operating of the system and is given by a nonlinear state-space representation. Whereas the previous works on fault diagnosis via sparse recovery techniques consider the static case only, the SRD method allows to take into account operating faults that depend on time and/or state. This is one of its most important characteristics.

The sparsity concept is introduced by the fact that the number of faults considered in the system modeling is much greater than the number of monitoring sensors as well as by the simultaneous appearance of the faults. This means that only a restricted number among the modeled faults can appear simultaneously. This number depends essentially on the number of monitoring sensors. Indeed, the SRD method takes into account a very large number of possible faults that may act on the system, but it can be applied under the assumption that few of them can occur simultaneously in the system. This can be seen as a limitation of the method but it can be overcome by increasing the number of monitoring sensors (thus by adding new sensors) allowing to obtain more system information and, therefore, to diagnose more defects.

Another important point is that the SRD is an on line diagnosis method (where by

on line we mean that all algorithms are solved in a continuous process and with the same computation step).

Since the SRD method is based on a state-space representation, it belongs to the class of model-based diagnosis methods. In the literature, many works apply or develop model-based techniques in order to diagnose different faults (see , for instance, [29], [12], [44]). Very often they are based on residuals generation for the state variables or/and the output variables. The created residuals represent, in general, the difference between the estimated healthy variables and the real ones. These methods allow to diagnose faults by checking the consistency between this difference and a threshold that is fixed to distinguish the healthy from the faulty operating of the system or by applying some temporal and/or frequency analysis. However, in some complex systems, model-based methods require high amount of measurements and computational efforts due to the existence of a large number of variables. Moreover, each fault should have its own diagnosis algorithm to be analyzed, detected and isolated, in particular, when similarities between different residuals occur. This may render the system even more complex or may lead to dealing with big-data problems in the case of many various faults. From this point of view, a main advantage of the SRD method is that it allows to consider many different faults in the system modeling and, moreover, their diagnosis is carried out by an on line diagnosis algorithm with finite-time convergence. Furthermore, the SRD method allows to detect, locate and isolate faults using a single algorithm. This is not always possible for others diagnosis methods (because of a difficult localization step that requires some specific knowledge of the system characteristics, due to the lack of the algebraic relations between different system variables).

To sum up, with the help of the SRD method, a complete diagnostic (detection, location and identification) can be obtained. To illustrate its performances, we apply it to diagnose faults in a gearbox system.

The gear power transmission has a crucial role in mechanical transmission systems and its diagnosis depends on how faults affect the system. Some faults (like misalignment, eccentricity) may produce amplitude modulations. On the other hand, frequency modulations can be caused by other types of faults (such as gears cracking or flaking). Therefore, sometimes it may be difficult to identify the nature of the defects.

The gearbox system considered in this paper is composed by a two-stage gear and is affected by different mechanical and sensor faults. With the help of the SRD method, detection, identification and localization of the system faults are carried out. The simulation results show the accurate reconstruction of the mechanical faults and their diagnostic is carried out by verifying the nature of the obtained defect signal and by using some frequential/temporal characteristics of the gear elements.

The paper is organized as follows: the next section is devoted to the general presentation of the SRD method. Then, in the third section, we present the healthy and faulty models of the gear power transmission system and explain how the SRD method can be applied for this particular dynamical systems. The fourth section shows simulations results implemented on Matlab/Simulink and discusses the good performances of the SRD method. Finally, some conclusions are presented.

2 Sparse recovery diagnosis method

3 Problem statement

Table 1: Principal notations

Name	Description
x	State vector
$f(x)$	Nonlinear dynamics of the system
$g_j(x)$	Nonlinear dynamics of the faults
w_j	jth operating fault, $1 \leq j \leq p$
y_i	Measurement output, $1 \leq i \leq m$
$h_i(x)$	Function of the measurement output, $1 \leq i \leq m$
s_i	Fault of the ith sensor, $1 \leq i \leq m$
n	Dimension of the system state
m	Number of monitoring sensors
p	Number of system faults
q	Total number of faults ($q = p + m$)
ρ_i	Relative degree of the output y_i
Φ	Matrix information
χ	Measurement vector
$d(t)$	Fault vector
s	Number of simultaneously occurring faults
λ	Balancing parameter
α	Exponential coefficient
$L_f^\ell h_i$	ℓth-order Lie derivative of the function h_i along the vector field f

Consider the following nonlinear state-space representation describing the healthy operating mode of the system:

$$\begin{cases} \dot{x} = f(x) \\ y_i = h_i(x), 1 \leq i \leq m. \end{cases} \tag{1}$$

where $x \in \mathbb{R}^n$ is the state vector, $f(x)$ is the nonlinear dynamics, $y \in \mathbb{R}^m$ is the m-dimensional measurement output (corresponding to the sensor outputs). The point denotes the derivative with respect to an independent variable which in general represents the time. The functions h_i, for $1 \leq i \leq m$, are supposed independent.

The appearance of faults in physical systems is often an inevitable phenomenon that, in general, modifies their dynamical behavior. They are modeled by the following extension of representation (1):

$$\begin{cases} \dot{x} = f(x) + \sum_{j=1}^{p} g_j(x) w_j(t), \\ y_i = h_i(x) + s_i, 1 \leq i \leq m. \end{cases} \tag{2}$$

where $(w_1(t), \cdots, w_p(t))^T$ and $(s_1, \cdots, s_m)^T$ are vectors of, respectively, the system operating faults and the sensor faults. All $g_j(x)$, $1 \leq j \leq p$, are known vector fields related to the dynamics faults. We suppose that f, g_j and h_i are sufficiently smooth. All sensor faults s_i

are assumed piecewise-constant functions (explaining the lack of the t-argument in (2)) of the form:

$$s_i = \begin{cases} 0, \text{ if } 0 \leq t < t_i, \\ a_i, \text{ if } t \geq t_i, \end{cases} \tag{3}$$

for $1 \leq i \leq m$, with a_i the fault magnitude and t_i the appearance time of the fault.

The total number of faults $q = p + m$ is supposed much greater than the number of monitoring sensors (see Assumption 3.2). It is clear that if some faults are equal to zero (*i.e.*, $w_j = 0$, for some $1 \leq j \leq p$, or $s_i = 0$, for some $1 \leq i \leq m$), then those faults do not affect the system and thus they do not disrupt the operating of (2). The principal notations used in this section are recalled in Table 1.

Example 3.1. In order to illustrate the different notations required for the introduction of the SRD method, we consider the following system:

$$\begin{cases} \dot{x}_1 = x_2 + x_3 + 2x_3w_1 + x_3^2w_2, \\ \dot{x}_2 = 2x_3^2 + x_3x_1 + x_3w_2 + x_3w_3 + x_3w_4, \\ \dot{x}_3 = x_1 + x_4 + x_3w_2 + 2w_4, \\ \dot{x}_4 = x_2 + x_3^2 + x_3w_2, \end{cases} \tag{4}$$

with the measurements:

$$\begin{cases} y_1 = x_1 + x_2 + s_1, \\ y_2 = x_2 + s_2, \\ y_3 = x_4 + s_3, \end{cases} \tag{5}$$

where $x = (x_1\ x_2\ x_3\ x_4)^T \in \mathbb{R}^4$ is the state vector, $(w_1\ w_2\ w_3\ w_4)^T \in \mathbb{R}^4$ is the vector of operating faults, $(s_1\ s_2\ s_3)^T \in \mathbb{R}^3$ is the vector of sensor faults and

$$g_1 = \begin{pmatrix} 2x_3 \\ 0 \\ 0 \\ 0 \end{pmatrix}, \ g_2 = \begin{pmatrix} x_3^2 \\ x_3 \\ x_3 \\ x_3 \end{pmatrix}, \ g_3 = \begin{pmatrix} 0 \\ x_3 \\ 0 \\ 0 \end{pmatrix}, \ g_4 = \begin{pmatrix} 0 \\ x_3 \\ 2 \\ 0 \end{pmatrix}$$

are the vector fields showing how the operating faults w_j act on the system. Notice that they are state dependent. ▲

In order to apply the SRD method, it is important to work in coordinates in which each output corresponds to one (and only one) state variable of the system. Hence, the following change of coordinates may be required: introduce $\tilde{x} = \varphi(x) \in \mathbb{R}^n$, where $\varphi(x)$ is a local diffeomorphism whose m first components are given by $\varphi_i(x) = h_i(x)$ and the last $n - m$ are any original coordinates completing the functions h_i, $1 \leq i \leq m$, to a coordinate system. Notice that the local diffeomorphism $\varphi(x)$ always exists. In the new coordinates, system (2) can be written as:

$$\begin{cases} \dot{\tilde{x}} = \tilde{f}(\tilde{x}) + \sum_{j=1}^{p} \tilde{g}_j(\tilde{x})w_j(t), \\ y_i = \tilde{x}_i + s_i, 1 \leq i \leq m, \end{cases} \tag{6}$$

with

$$\tilde{f}(\tilde{x}) = \frac{\partial \varphi}{\partial x}(x) \cdot f(x) = \frac{\partial \varphi}{\partial x}(\varphi^{-1}(\tilde{x})) \cdot f(\varphi^{-1}(\tilde{x})),$$

and

$$\tilde{g}_j(\tilde{x}) = \frac{\partial \varphi}{\partial x}(x) \cdot g_j(x) = \frac{\partial \varphi}{\partial x}(\varphi^{-1}((\tilde{x})) \cdot g_j(\varphi^{-1}(\tilde{x})),$$

where φ^{-1} is the local inverse of $\varphi(x)$. Observe that in the new $\tilde{x}$-coordinates, the measurements are simply the m first states $\tilde{x}_i$, $1 \leq i \leq m$. Notice that for mechanical systems, this is often the case since usually we measure the states of the system (displacements, rotational speed, *etc*). In order to simplify the notation, from now on, we will drop the tildes.

We denote the total number of faults by q (that is, $q = m + p$) and define the following global fault vector including the defects affecting both the dynamics and the sensors:

$$d(t) = \begin{pmatrix} s_1 \\ \vdots \\ s_m \\ w_1(t) \\ \vdots \\ w_p(t) \end{pmatrix} \in \mathbb{R}^q. \tag{7}$$

Example 3.1 (continuation)**.** For system (4) together with measurements (5), the diffeomorphism $\varphi(x)$ can be taken as:

$$\begin{cases} \tilde{x}_1 = x_1 + x_2, \\ \tilde{x}_2 = x_2, \\ \tilde{x}_3 = x_4, \\ \tilde{x}_4 = x_3, \end{cases} \tag{8}$$

with inverse

$$\begin{cases} x_1 = \tilde{x}_1 - \tilde{x}_2, \\ x_2 = \tilde{x}_2, \\ x_3 = \tilde{x}_4, \\ x_4 = \tilde{x}_3. \end{cases} \tag{9}$$

In the new $\tilde{x}$-coordinates we obtain:

$$\begin{cases} \dot{\tilde{x}}_1 = \tilde{x}_2 + \tilde{x}_4 + 2\tilde{x}_4^2 + (\tilde{x}_1 - \tilde{x}_2)\tilde{x}_4 + 2\tilde{x}_4 w_1 + (\tilde{x}_4^2 \\ \qquad +\tilde{x}_4)w_2 + \tilde{x}_4 w_3 + \tilde{x}_4 w_4, \\ \dot{\tilde{x}}_2 = 2\tilde{x}_4^2 + \tilde{x}_4(\tilde{x}_1 - \tilde{x}_2) + \tilde{x}_4 w_2 + \tilde{x}_4 w_3 + \tilde{x}_4 w_4, \\ \dot{\tilde{x}}_3 = \tilde{x}_1 - \tilde{x}_2 + \tilde{x}_3 + \tilde{x}_4 w_2 + 2w_4, \\ \dot{\tilde{x}}_4 = \tilde{x}_2 + \tilde{x}_4^2 + \tilde{x}_4 w_2, \end{cases} \tag{10}$$

with the measurements (notice that each output h_i corresponds to a new state variable $\tilde{x}_i$)

$$\begin{cases} y_1 = \tilde{x}_1 + s_1, \\ y_2 = \tilde{x}_2 + s_2, \\ y_3 = \tilde{x}_3 + s_3. \end{cases} \tag{11}$$

The global fault vector of (10)-(11) is defined by $d(t) = [s_1 \ s_2 \ s_3 \ w_1 \ w_2 \ w_3 \ w_4]^T \in \mathbb{R}^7$. ▲

Definition 3.1 ((Relative degree with respect to the operating faults)). The relative degree of the output component $h_i(x) = x_i$, $1 \leq i \leq m$, is the positive integer ρ_i defined as follows:

$$\begin{cases} L_{g_j} L_f^{\ell} h_i = 0, \text{ for all } 0 \leq \ell < \rho_i - 2, 1 \leq j \leq p, \\ L_{g_j} L_f^{\rho_i - 1} h_i \neq 0, \text{ for some } 1 \leq j \leq p, \end{cases} \tag{12}$$

where $L_f^{\ell} h_i$ denotes the ℓth-order Lie derivative of the function h_i along the vector field f (see Definition 3.2 below).

Definition 3.2 ((Lie derivative)). The Lie derivative of the function h_i, $1 \leq i \leq m$, along a vector field f can be computed by:

$$L_f h_i(x) = \frac{\partial h_i(x)}{\partial x} \cdot f(x).$$

Recursively, we can define, for $\ell \geq 1$, the ℓth-order Lie derivative by:

$$L_f^{\ell} h_i(x) = L_f(L_f^{\ell-1} h_i(x)) = \frac{\partial L_f^{\ell-1} h_i(x)}{\partial x} \cdot f(x),$$

where $L_f^0 h_i(x) = h_i(x)$.

Hence, the term $L_{g_j} L_f^{\ell} h_i$ of (12) means

$$L_{g_j} L_f^{\ell} h_i(x) = \frac{\partial L_f^{\ell} h_i(x)}{\partial x} \cdot g_j(x).$$

Based on Definition 3.1, the relative degree ρ_i with respect to the operating faults can be calculated for each h_i. The integer ρ_i indicates the number of times that we have to differentiate before the effect of the operating faults can be seen on the output components h_i. In other words, ρ_i is the order of the first derivative of h_i that explicitly involves some of the operating faults w_j and provides information of w_j that will be used to detect them. Indeed, recall that $y_i = h_i(x) + s_i = x_i + s_i$, for $1 \leq i \leq m$ (see (3)), where all s_i are piecewise-constants thus, by Definition 3.1, for $1 \leq i \leq m$, we have:

$$y_i^{(\rho_i)} = L_f^{\rho_i} h_i(x) + \sum_{j=1}^{p} (L_{g_j} L_f^{\rho_i - 1} h_i(x)) w_j(t). \tag{13}$$

In order to extract the sensor faults, we replace the states x_i, for $1 \leq i \leq m$, in (13) by their measured values $y_i = x_i + s_i$ (the real measurements affected by the faults)

$$y_i^{(\rho_i)} = L_f^{\rho_i} h_i(y, \bar{x}) + \sum_{j=1}^{p} (L_{g_j} L_f^{\rho_i - 1} h_i(y, \bar{x})) w_j(t), \tag{14}$$

where $\bar{x}$ denotes the unmeasured states $\bar{x} = (x_{m+1}, \ldots, x_n)$.

Notice that expression (14) now involves explicitly s_i (via y_i) and this dependence may be nonlinear. In this paper, we treat only the case when the right-hand side of (14) is affine with respect to s_i, $1 \leq i \leq m$, (i.e., of form (15)). This assumption may seen restrictive, but if (14) is nonlinear with respect to s_i, then a Taylor approximation of the first order can be used (see [39]). With this assumption, (14) can be written as follows:

$$y_i^{(\rho_i)} = L_f^{\rho_i} h_i(x) + \sum_{j=1}^{m} \sigma_{ij}(x) s_j + \sum_{j=1}^{p} (L_{g_j} L_f^{\rho_i - 1} h_i(x)) w_j(t). \tag{15}$$

Example 3.1 (continuation)**.** For system (10), we compute the Lie derivative of each h_i, for $1 \leq i \leq 3$, along the vector fields g_j, for $1 \leq j \leq 4$, and obtain $\rho_i = 1$, for $1 \leq i \leq 3$.

In order to extract the sensor faults, we replace the states $\tilde{x}_1$, $\tilde{x}_2$ and $\tilde{x}_3$ in (10) by their measured values given by (11). We obtain the following equations represented in form (15):

$$\begin{cases} \dot{y}_1 = L_f h_1(\tilde{x}) + \tilde{x}_4 s_1 + (1 - \tilde{x}_4) s_2 + 2\tilde{x}_4 w_1 + (\tilde{x}_4^2 \\ \qquad +\tilde{x}_4) w_2 + \tilde{x}_4 w_3 + \tilde{x}_4 w_4, \\ \dot{y}_2 = L_f h_2(\tilde{x}) + \tilde{x}_4 s_1 - \tilde{x}_4 s_2 + \tilde{x}_4 w_2 + \tilde{x}_4 w_3 + \tilde{x}_4 w_4, \\ \dot{y}_3 = L_f h_3(\tilde{x}) + s_1 - s_2 + s_3 + \tilde{x}_4 w_2 + 2w_4, \end{cases} \tag{16}$$

where $L_f h_i$, for $1 \leq i \leq 3$, is the healthy operating dynamics of the system expressed in (10). ▲

Denote by χ the measurement vector:

$$\chi = \begin{pmatrix} y_1^{(\rho_1)} - L_f^{\rho_1} h_1 \\ \vdots \\ y_m^{(\rho_m)} - L_f^{\rho_m} h_m \end{pmatrix} \in \mathbb{R}^m. \tag{17}$$

Physically, $\chi \in \mathbb{R}^m$ represents the difference between the estimated time-derivatives of the measurements y_i and, the known dynamics of the healthy system. These derivatives can always be estimated if the system is observable with respect to the outputs $y_i = h_i(x)$, which is guaranteed by the observability assumption below (see Assumption 3.1).

Observability is a measure of how well internal states of the system can be inferred from knowledge of its external outputs [26]. A system is said to be observable if one can determine the behavior of the entire system from its measurements and eventually from the known inputs. More precisely, the current state values can be determined in finite-time using only the outputs (we send the reader to [26] for different notions of observability and formal definitions). If a system is not observable, this means that the current values of some of its state variables cannot be determined through output sensors. So observability can been seen as the ability to create enough smart sensors in order to recover all states of the system. The definition of observability as well as the criteria for checking it uses the state-space representation. To system (2), we associate the coditribution

$$\mathcal{O}(x) = \text{span}\{\mathrm{d}L_f^j h_i(x), 1 \leq i \leq m, j \geq 0\}.$$

System (2) is locally observable with respect to its outputs $y_i = h_i(x)$, $1 \leq i \leq m$, if locally

$$\dim \mathcal{O}(x) = n, \tag{18}$$

where n is the state-space dimension. This condition is called observability rank condition.

Assumption 3.1 ((Observability)). We assume that system (2) is observable with respect to the outputs $y_i = h_i(x)$, for $1 \leq i \leq m$, that is, it verifies the observability rank condition (18).

If the system is observable, dynamical equations can be designed to estimate the state of the system from the outputs measurements. Such module is called a state observer or simply an observer of the system. A state observer is typically computer-implemented and allows to fully reconstruct the system state from its output measurements. If derivatives of the output are required (as in our case, where we need $y_1^{\rho_i} \dots y_m^{\rho_m}$), then the term differentiator is used.

Since Assumption 3.1 is verified, nonlinear differentiators can be applied in order to estimate in finite-time the derivatives $(y_1^{(\rho_1)}, \cdots, y_m^{(\rho_m)})$, for more details, see [3], and thus to compute χ which plays an important role in the reconstruction (based on the measurements y_i and their derivatives) of the fault vector $d(t)$. Indeed, from relation (15), it follows that the vectors χ and $d(t)$ are related by an equation of the form:

$$\chi = \mathbf{\Phi}(x)d(t), \tag{19}$$

where $\mathbf{\Phi}(x)$ is the $(m \times q)$-matrix given by:

$$\mathbf{\Phi}(x) = \begin{pmatrix} \sigma_{11} \dots \sigma_{1m}\ L_{g_1}L_f^{\rho_1-1}h_1 & \dots L_{g_p}L_f^{\rho_1-1}h_1 \\ \vdots \quad\quad \vdots \quad\quad \vdots & \quad\quad\quad \vdots \\ \sigma_{m1} \dots \sigma_{mm} L_{g_1}L_f^{\rho_m-1}h_m & \dots L_{g_p}L_f^{\rho_m-1}h_m \end{pmatrix} \tag{20}$$

Example 3.1 (continuation). Based on (16), we deduce the measurement vector $\chi \in \mathbb{R}^3$:

$$\chi = \begin{pmatrix} \dot{y}_1 - L_f h_1(\tilde{x}) \\ \dot{y}_2 - L_f h_2(\tilde{x}) \\ \dot{y}_3 - L_f h_3(\tilde{x}) \end{pmatrix}, \tag{21}$$

and the matrix $\mathbf{\Phi}(x) \in \mathbb{R}^{3\times 7}$:

$$\mathbf{\Phi}(x) = \begin{pmatrix} \tilde{x}_4 & (1-\tilde{x}_4) & 0 & 2\tilde{x}_4 & (\tilde{x}_4^2 + \tilde{x}_4) & \tilde{x}_4 & \tilde{x}_4 \\ \tilde{x}_4 & -\tilde{x}_4 & 0 & 0 & \tilde{x}_4 & \tilde{x}_4 & \tilde{x}_4 \\ 1 & -1 & 1 & 0 & \tilde{x}_4 & 0 & 2 \end{pmatrix}. \tag{22}$$

▲

Equation (19) will be used to recover the unknown faults from the measurements information. Indeed, the goal of the fault detection problem is to solve the algebraic system of m equations, given by (19), with q unknowns, *i.e.*, the components of the fault vector $d(t) \in \mathbb{R}^q$. This problem is well known as a left invertibility problem (see, for instance, [37], [35], [36]).

The left invertibility problem has been widely studied and applied to many different problems (going from fault diagnosis [33] to cryptographic applications [40], *etc*). It consists in determining the causal factors (*i.e.,* the unknown inputs signals or, like in our context, the fault vector) from the knowledge of a set of observations (*i.e.,* the measurement outputs and its derivatives). In the case when $q \leq m$ (*i.e.,* the number of measurements is greater or equal than the number of the unknown inputs corresponding to the faults), the inverse problem can be solved either by inverting, if possible, directly the matrix $\mathbf{\Phi}(x)$ (when $m = q$ and $\mathbf{\Phi}(x)$ invertible) or by solving the system of equations based on the dimension reduction (if $m > q$). In the over complete matrix (when $m < q$, which is usually the case in the context of fault detection), the left invertibility problem either has no solution or has an infinity of

solutions. However, if the vector d is sparse, then, in the particular case when relation (19) is static, that is, the matrix $\mathbf{\Phi}$ and the fault vector d are constant (do not depend on time or state) reconstruction strategies enabling to exactly reconstruct the unknown signal and can be deployed (see, for example, [6], [41]).

In the context of fault detection, techniques based on sparse recovery methods have already been developed (see for example, [38], [19]) with the particularity that the faults are not introduced mathematically in the system and their features are recovered from the frequency content in which the most coefficients are sparse (for instance, using Fourier or wavelet transforms). Therefore, the originality of our work is firstly, to apply the SRD method in the dynamical case (that is, when $\mathbf{\Phi}(x)$ and $d(t)$ depend on time or state) and secondly, to consider a system modeling based on a state-space representation that describes the healthy and the faulty behavior.

Another particularity of the SRD method is that all algorithms (corresponding to the optimization problem given by (30) and to the observers equations, see, for instance [25], [3], [15]) are solved in a continuous process (that is, in the same iteration loop) and with the same computation step. In other words, with the help of a single simulation of all algorithms, the diagnostic of numerous different faults is obtained which is not always possible for other diagnostic methods (that often require several analyzes to be able to diagnose different faults).

Remark 3.1. One of the difficulties when adapting the sparse recovery method to nonlinear dynamical systems is the fact that the matrix $\mathbf{\Phi}(x)$ is state dependent and moreover, its choice is not always unique, as explained below. Indeed, very often, when modeling the system, the vector $d(t)$ includes as much information as possible related to the faults, that is, the fault signatures w_j (*i.e.,* the quantity that is always zero when the operating system is healthy, and is nonzero when the corresponding fault acts on the system) as well as for each w_j the common terms to all components of the vector g_j through which the fault w_j acts on the system. But $d(t)$ can also be defined with the help of the signatures w_j only (like in expression (7)). So for nonlinear dynamical systems, the choice of the fault vector $d(t)$, and, therefore, of the matrix $\mathbf{\Phi}(x)$ is not unique. The choice of $\mathbf{\Phi}(x)$ is crucial for the SRD method. Indeed, $\mathbf{\Phi}(x)$ has to satisfy some theoretical conditions (namely, the RIP condition that will be defined below, see Definition 3.4). If the matrix $\mathbf{\Phi}(x)$ constructed in the classical way, does not verify that condition, some constant or variable coefficients can be transferred from the vector $d(t)$ to the matrix $\mathbf{\Phi}(x)$ without loss of information on the fault vector (since we always keep in $d(t)$ the fault signatures as explained above).

Example 3.1 (continuation)**.** Consider now the global fault vector $d(t)=[s_1\ s_2\ s_3\ w_1\ w_2\ \tilde{x}_4 w_3\ w_4]^T \in \mathbb{R}^7$ (notice that its $6th$ component contains the signature w_3 of the fault as well as the term $\tilde{x}_4$ which is common to all $\tilde{g}_3$ components, see (10)). Its associated matrix $\mathbf{\Phi}(x)$ is given by:

$$\mathbf{\Phi} = \begin{pmatrix} \tilde{x}_4 & (1-\tilde{x}_4) & 0 & 2\tilde{x}_4 & (\tilde{x}_4^2+\tilde{x}_4) & 1 & \tilde{x}_4 \\ \tilde{x}_4 & -\tilde{x}_4 & 0 & 0 & \tilde{x}_4 & 1 & \tilde{x}_4 \\ 1 & -1 & 1 & 0 & \tilde{x}_4 & 0 & 2 \end{pmatrix}. \tag{23}$$

▲

The goal of the SRD method is to reconstruct a sparse fault vector $d(t)$ based on the measurement outputs y_i, $1 \leq i \leq m$, and their derivatives. The term sparse means that the dimension q of $d(t)$ may be very large (*i.e.,* there are many possible faults that are taken into

account in the model), but only a few number of components may be non zero (*i.e.,* only few faults act simultaneously on the system). In other words, the objective of this method is to reconstruct the most parsimonious solution of the fault vector $d(t)$ with the help of the measurements vector χ and the matrix $\mathbf{\Phi}(x)$ (*i.e.,* where by most parsimonious, we mean the solution with the lowest number of non-zero components of $d(t)$). This can be reformulated as the following optimization problem ([5], [7], [4]):

$$\min_{d\in\mathbb{R}^q}\|d\|_0, \quad \text{under the constraint} \quad \chi = \mathbf{\Phi}(x)d(t), \tag{24}$$

where $\|d\|_0$ is a pseudo-norm and corresponds to the number of non-zero values of $d(t)$.

An equivalent description of problem (24) is to minimize a cost function constructed by leveraging the observation error $\chi - \mathbf{\Phi}(x)d(t)$ by respecting the parsimony constraint on $d(t)$ via a balancing parameter λ (see, for example, [7]):

$$\min_{d\in\mathbb{R}^q}\{\frac{1}{2}\|\chi - \mathbf{\Phi}(x)d(t)\|_2^2 + \lambda\|d(t)\|_0\}. \tag{25}$$

The optimization problem (25) is N.P-complete, thus difficult to solve (since the pseudo-norm zero is non-differentiable). But if the matrix $\mathbf{\Phi}(x)$ satisfies the Restricted Isometry Property (RIP) recalled below, then problem (25) can be transformed into an equivalent one where the pseudo-norm $\|.\|_0$ is replaced by the norm $\|.\|_1$. Before giving the RIP definition, we need the notion of s-sparsity.

Definition 3.3 (sparsity)**.** The fault vector $d(t)$ is s-sparse if at most s non-zero faults can appear simultaneously. The non-zero faults are called active faults or active nodes.

Notice that $d(t)$ is s-sparse means that among the $q = m+p$ modeled faults only s of them may act on the system. Recall that the number q of the total faults is much greater than s which in turn is smaller than m. For the SRD method, we need the following assumption:

Assumption 3.2 (s-sparsity of the fault vector)**.** We assume that $d(t)$ is s-sparse and, moreover that s verifies the following condition:

$$2s + 1 \leq m. \tag{26}$$

Definition 3.4 (s-order RIP condition)**.** A matrix $\mathbf{\Phi}(x)$ is said to satisfy the s-order RIP condition, if for any s-sparse signal $d(t)$, the following condition is verified:

$$(1 - \delta_s)\|d\|_2^2 \leq \|\mathbf{\Phi}(x)d(t)\|_2^2 \leq (1 + \delta_s)\|d\|_2^2, \tag{27}$$

where $\delta_s \in (0, 1)$ is a constant parameter. This property will be called the s-order RIP condition.

In order to check if a matrix $\mathbf{\Phi}(x)$ satisfies the s-order RIP condition, let Γ denote any set of s indices among 1 to q (where q is the total number of faults), *i.e.,* Γ is any s-combination of the set $\{1, 2, \ldots, q\}$. Notice that Γ is not unique and there are $\frac{q!}{s!(q-s)!}$ of them. Denote by $\mathbf{\Phi}_\Gamma(x)$ the sub-matrix of $\mathbf{\Phi}(x)$ formed by the columns of $\mathbf{\Phi}(x)$ indexed by the elements of the set Γ (*i.e.,* corresponding to the active nodes s) and by $\mathbf{\Phi}_\Gamma^T(x)$ its transposed matrix. The s-order RIP condition for a matrix $\mathbf{\Phi}(x)$ is equivalent to the fact that all eigenvalues of the matrix product $\mathbf{\Phi}_\Gamma^T(x)\mathbf{\Phi}_\Gamma(x)$, for all possible s-combinations Γ, must be strictly between 0 and 2, that is:

$$1 - \delta_s \leq eig(\mathbf{\Phi}_\Gamma^T(x)\mathbf{\Phi}_\Gamma(x)) \leq 1 + \delta_s \tag{28}$$

for $\delta_s \in (0, 1)$.

Remark 3.2. Recall that the matrix $\mathbf{\Phi}(x)$ associated to system (2) and to fault vector (7) is not unique and its expression depends on the definition of $d(t)$, see Remark 3.1. If no matrix $\mathbf{\Phi}(x)$ (constructed using the procedure of Remark 3.1) verifies the s-order RIP condition, we choose one of them and try to transform it in such a way that this property is satisfied for the transformed matrix. We explain next how to do it. First, notice that if the RIP condition is satisfied then all sub-matrices $\mathbf{\Phi}_\Gamma(x)$ are of full rank. Thus we have to eliminate the columns of the original matrix $\mathbf{\Phi}(x)$ that are identical or proportional. In this case, their corresponding faults act in the same way on the system and they can be emerged by adding them and eliminating one of the columns.

For instance, if the first column $\mathbf{\Phi}_1$ of $\mathbf{\Phi}(x)$ (corresponding to $d_1(t)$) and the second one $\mathbf{\Phi}_2$ (corresponding to $d_2(t)$) are like above (*i.e.,* $\mathbf{\Phi}_1 = \mathbf{\Phi}_2$ or $\mathbf{\Phi}_1 = a\mathbf{\Phi}_2$ where a is a constant or a functional parameter), we will keep only one of them (say the first one) and its new associated fault becomes $d_1(t) + d_2(t)$ if $\mathbf{\Phi}_1 = \mathbf{\Phi}_2$, respectively, $d_1(t) + ad_2(t)$, if $\mathbf{\Phi}_1 = a\mathbf{\Phi}_2$. Remark that by regrouping the faults, the dimension of the global fault vector $d(t)$ decreases from q to $q-1$. After this procedure the dimensions of $\mathbf{\Phi}(x)$ change as well (the number of columns decreases, but the number of lines remains unchanged) and the new matrix $\mathbf{\Phi}(x)$ no longer contains identical or proportional columns (this does not mean that $\mathbf{\Phi}(x)$ is of full rank, in fact, $\mathbf{\Phi}(x)$ may possess columns that are linear combinations of at least two other columns. If the transformed matrix $\mathbf{\Phi}(x)$ still does not verify the RIP condition, we start to eliminate those collinear columns and apply the same principle to regroup the corresponding faults (for instance, if $\mathbf{\Phi}_1 = a\mathbf{\Phi}_2 + b\mathbf{\Phi}_3$, where a and b are constant or functional parameters, we keep $\mathbf{\Phi}_2$ and $\mathbf{\Phi}_3$, but eliminate $\mathbf{\Phi}_1$, the new faults corresponding to $\mathbf{\Phi}_2$ and $\mathbf{\Phi}_3$ being $d_2(t) + ad_1(t)$ and $d_3(t) + bd_1(t)$). After each such column removal, we check if the new matrix $\mathbf{\Phi}(x)$ verify the s-order RIP condition.

In order to check the s-order RIP condition, it may also be helpful to normalize each column of the matrix $\mathbf{\Phi}(x)$ with respect to the norm $\|\cdot\|_2$ (after normalization, we should have $\|\mathbf{\Phi}_k(x)\|_2 = \sqrt{\sum_{i=1}^{m} |\mathbf{\Phi}_{ik}(x)|^2} = 1$, $1 \leq k \leq q$, where $\mathbf{\Phi}_k$ denotes the kth column of $\mathbf{\Phi}$). As a consequence of this normalization, each component of the fault vector has to be multiplied by the norm of its corresponding column in $\mathbf{\Phi}(x)$. In some cases, the normalization of the matrix $\mathbf{\Phi}(x)$ is not necessary to verify the s-order RIP condition (there are matrices verifying this condition whose columns are not normalized).

In the sequel, we continue to denote the transformed matrix by $\mathbf{\Phi}(x)$, the new fault vector by $d(t)$ and its number components by q. Suppose that:

Assumption 3.3. (s-order RIP) The transformed matrix $\mathbf{\Phi}(x)$ is assumed to satisfy the s-order RIP condition.

Under Assumption 3.3, the parsimony problem (25) for the transformed matrix $\mathbf{\Phi}(x)$ and the new fault vector $d(t)$ becomes:

$$\min_{d \in \mathbb{R}^q} \{\frac{1}{2}\|\chi - \mathbf{\Phi}(x)d(t)\|_2^2 + \lambda\|d(t)\|_1\}, \tag{29}$$

and its solution exists and is unique [42].

Recall that $m < q$ (*i.e.,* the number of monitoring sensors is significantly smaller than the number of faults) and in general, even after transforming the original matrix $\mathbf{\Phi}(x)$, when necessary, we still have $m < q$, where q denotes now the dimension of the new regrouped fault vector, thus, $\mathbf{\Phi}(x)$ cannot be invertible (since the matrix is not square) and, the left

invertibility cannot be applied. Nevertheless, under Assumptions 3.2 and 3.3, the fault vector $d(t)$ can be detected and reconstructed as a solution of (29). To that end, the following dynamical algorithm based on sliding mode techniques [21] is proposed reminding very much that of [42] with the difference that the matrix $\mathbf{\Phi}$ and the vector d are no longer constant (see also [1] for the linear case):

$$\begin{cases} \tau \dot{u}(t) = -\lceil u(t) + (\mathbf{\Phi}^T(x)\mathbf{\Phi}(x) - Id)\hat{d}(t) - \mathbf{\Phi}^T(x)\chi \rfloor^{\alpha}, \\ \hat{d}(t) = \varphi_{\lambda}(u(t)), \end{cases} \tag{30}$$

where $\lceil . \rfloor^{\alpha} = |.|^{\alpha} sign(.)$, $u(t) \in \mathbb{R}^q$ is the internal state vector, $\varphi_{\lambda}(u(t)) = \max(|u| - \lambda, 0) sign(u)$ is the continuous soft thresholding function, $\lambda \in \mathbb{R}^q$ is a vector of constant positive parameters that has to be suitably chosen in function of the noise and the minimum possible absolute values of the faults, the vector $\hat{d}(t)$ represents the estimation of the sparse signal $d(t)$, τ is a $(q \times q)$-diagonal matrix with constant parameters $\tau_i, 1 \leq i \leq q$, determined by the physical properties of the implementing system, Id is the identity $(q \times q)$-matrix and the exponential coefficient α is such that $\alpha \in [0, 1]$. In [42], it has been proven, in the case when the matrix $\mathbf{\Phi}(x)$ and the vector $d(t)$ are constant, that under Assumptions 3.2 and 3.3 and for $\alpha \in [0, 1)$, the state u converges, in finite-time, to its equilibrium point and thus the estimated fault vector $\hat{d}(t)$ converges in finite-time to $d(t)$. For $\alpha = 1$, only asymptotic convergence is ensured. If $\mathbf{\Phi}(x)$ and $d(t)$ depend explicitly on time or/and states, when adapting the proof of [42] to this dynamical case, the derivatives of $\mathbf{\Phi}(x)$ and $d(t)$ appear and have to be crushed with a suitable choice of λ. In this case, a practical stability can be guaranteed (see [8] for more details).

Remark 3.3. In the case when different faults are regrouped, the estimated fault vector $\hat{d}(t)$ converges to the new fault vector $d(t)$ (with regrouped faults). If one of the component of $\hat{d}(t)$ corresponding to some regrouped original faults (say $d_1(t) + d_2(t)$) is non zero, this means that $d_1(t)$ or $d_2(t)$ or both of them are activated. If only one fault among $d_1(t)$ and $d_2(t)$ is activated, in general, the faults diagnosis is possible either by verifying the order of magnitude of the defect or by the type of the obtained fault signal. However, if the two added faults are activated simultaneously, the estimated fault vector given by the SRD method contains the sum of these two faults and we may not be able to identify or to localize them. These situations will be discussed in our case study in the next section.

Remark 3.4. In some cases, the dynamics f and/or vector fields g_j can depend explicitly on time (*i.e.,* we have $f = f(t, x(t))$ and/or $g_j = g_j(t, x(t))$, for some $1 \leq j \leq p$). Thus the system is a time-variant one. A classic way to transform it into a time-invariant system (that is, of form (2)) is to introduce an additional state (which is simply the time-variable) described by the equation:

$$\dot{x}_{n+1}(t) = 1. \tag{31}$$

The associated extended system is time-invariant and contains $n+1$ states variables $\begin{pmatrix} x \\ x_{n+1} \end{pmatrix} \in \mathbb{R}^{n+1}$. The new dynamics is $\begin{pmatrix} f(x, x_{n+1}) \\ 1 \end{pmatrix}$ and the vector fields associated to the faults are $\begin{pmatrix} g_j(x, x_{n+1}) \\ 0 \end{pmatrix}$, for $1 \leq j \leq p$. Moreover t is, in general, also an output (or, at least, a known state) of the system.

4 Case Study

Table 2: Nomenclature of the two-stage gear system

Name	Description	Unit
θ_i	Angular position of the ith gear	[rad]
R_i	Bases radius of the ith gear	[m]
I_i	Inertia moment of the ith gear	[kg $\times$ m^2]
I_s	Inertia moment of the shaft	[kg $\times$ m^2]
$k_e(t)$	Time dependent gear-mesh stiffness	[N/m]
k_s	Torsional stiffness of the shaft	[N $\times$ m/rad]
$\mathfrak{q}$	Vector of degrees of freedom	[rad]
F	External torques vector	[N $\times$ m]
F_{1ec}	Eccentricity fault vector	[N $\times$ m]
F_c	Crack fault vector	[N $\times$ m]

In this section, we will apply the SRD method to diagnose mechanical faults in a gear power transmission system. The considered system is a reduced model of two-stage gear that takes into account only four degrees of freedom (see Figure 1). The principal notations used in the system modeling are recalled in Table 2.

4.1 Healthy model

The healthy system (see Figure 1) is composed of two pinions and two wheels supported by three shafts, one for the input shaft (the motor), the second for the intermediate shaft (which connects both stages of the gearbox system) and the third for the output shaft (the load). The model is obtained by developing the Lagrange equations of the kinetic and potential energies corresponding to the two-stage gear (see also [20] and [14] for a single stage modelisation).

The Lagrange formalism leads to the set of differential equations governing the system motion:

$$\mathbf{M}\ddot{\mathfrak{q}} + \mathbf{C}\dot{\mathfrak{q}} + \mathbf{K}(t)\mathfrak{q} = F, \tag{32}$$

where $\mathfrak{q}$ is the vector of degrees of freedom $\mathfrak{q} = [\theta_1\ \theta_2\ \theta_3\ \theta_4]^t$, $\mathbf{M}$ is the mass matrix expressed by:

$$\mathbf{M} = \begin{bmatrix} I_1 & 0 & 0 & 0 \\ 0 & I_2 + I_s & 0 & 0 \\ 0 & 0 & I_3 + I_s & 0 \\ 0 & 0 & 0 & I_4 \end{bmatrix}, \tag{33}$$

with I_i the inertia moment of the ith gear, $1 \leq i \leq 4$, and I_s the inertia moment of the intermediate shaft, $\mathbf{C}$ the damping, F the applied forces vector $F = [C_m\ 0\ 0\ C_r]^T$, where C_r and C_m are, respectively, the load and the motor torques of the system and $\mathbf{K}(t)$ presents the time-varying stiffness matrix containing the gear-mesh stiffness matrix $\mathbf{K}_e(t)$ and the constant shaft torsional stiffness matrix $\mathbf{K}_s$:

$$\mathbf{K}(t) = \mathbf{K}_e(t) + \mathbf{K}_s. \tag{34}$$

The gear-mesh stiffness matrix $\mathbf{K}_e(t)$ is defined by :

$$\mathbf{K}_e(t) = \begin{bmatrix} k_1(t)c^2R_1^2 & k_1(t)c^2R_1R_2 & 0 & 0 \\ k_1(t)c^2R_1R_2 & k_1(t)c^2R_2^2 & 0 & 0 \\ 0 & 0 & k_2(t)c^2R_3^2 & k_2(t)c^2R_3R_4 \\ 0 & 0 & k_2(t)c^2R_4R_3 & k_2(t)c^2R_4^2 \end{bmatrix}, \tag{35}$$

where R_i, $1 \leq i \leq 4$, represents the base radius of the ith gear and $k_j(t)$, $j = 1, 2$, is the time-varying stiffness for the jth stage defined as a square wave depending on time. The constant c simply denotes $c = \cos(\beta)$, with β the helix angle of the gears.

The shaft torsional stiffness matrix $\mathbf{K}_s$ is expressed as:

$$\mathbf{K}_s = \begin{bmatrix} 0 & 0 & 0 & 0 \\ 0 & k_s & -k_s & 0 \\ 0 & -k_s & k_s & 0 \\ 0 & 0 & 0 & 0 \end{bmatrix}, \tag{36}$$

where k_s is the constant torsional stiffness of the shaft.

Developing (32), we obtain the following state-space representation of the two-stage gearbox model:

$$\begin{cases} \dot{\theta}_1 = \Omega_1, \\ \dot{\theta}_2 = \Omega_2, \\ \dot{\theta}_3 = \Omega_3, \\ \dot{\theta}_4 = \Omega_4, \\ \dot{\Omega}_1 = \frac{1}{I_1}[-K_{11}\theta_1 - K_{12}\theta_2 - C_{11}\Omega_1 - C_{12}\Omega_2 + C_m], \\ \dot{\Omega}_2 = \frac{1}{I_2+I_s}[-K_{21}\theta_1 - K_{22}\theta_2 - K_{23}\theta_3 - C_{21}\Omega_1 \\ \qquad -C_{22}\Omega_2 - C_{23}\Omega_3], \\ \dot{\Omega}_3 = \frac{1}{I_3+I_s}[-K_{32}\theta_2 - K_{33}\theta_3 - K_{34}\theta_4 - C_{32}\Omega_2 \\ \qquad -C_{33}\Omega_3 - C_{34}\Omega_4], \\ \dot{\Omega}_4 = \frac{1}{I_4}[-K_{43}\theta_3 - K_{44}\theta_4 - C_{43}\Omega_3 - C_{44}\Omega_4 + C_r], \end{cases} \tag{37}$$

where K_{ij} and C_{ij}, for $1 \leq i, j \leq 4$, are respectively, the coefficients of the stiffness matrix $\mathbf{K}(t)$ and damping matrix $\mathbf{C}$, $[\theta\ \Omega]^T \in \mathbb{R}^8$ is the state vector whose components are the degrees of freedom of the system.

For (37), we have the following measurements:

$$\begin{aligned} y_1 &= \theta_1, \\ y_2 &= \theta_2, \\ y_3 &= \theta_3, \\ y_4 &= \theta_4. \end{aligned} \tag{38}$$

4.2 Faulty model

In this paper, we suppose that mechanical faults and sensor faults can affect the gearbox system. We model two types of mechanical faults: eccentricity and crack defects. The faulty model is given by the following equation of motion

$$\mathbf{M}\ddot{\mathfrak{q}} + \mathbf{C}\dot{\mathfrak{q}} + \mathbf{K}(t)\mathfrak{q} = F + F_{ec} + F_c, \tag{39}$$

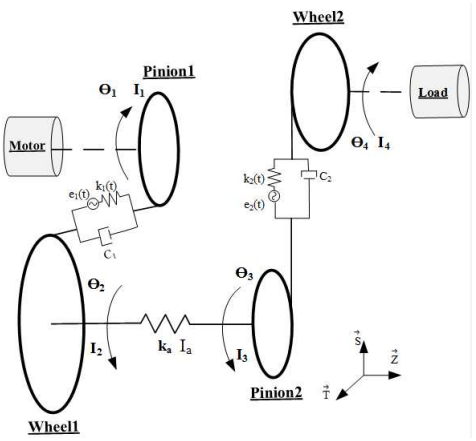

Figure 1: Torsional model of a two-stage gear

where F_{ec} and F_c, correspond, respectively, to the eccentricity and the crack defects.

The eccentricity fault is defined as the gap between the geometrical and the rotational axes of the gear. It is composed by two components: the first one F_{1ec} is related to a modification in the kinetic energy and the second one F_{2ec} is due to the change in potential energy:

$$F_{ec} = F_{1ec} + F_{2ec}. \tag{40}$$

We have:

- $F_{1ec} = [0 \;\; I_2\dot{\omega}_2 \;\; 0 \;\; I_4\dot{\omega}_4]^T$, where ω_i is the angular velocity of the ith gear given by $\omega_i = -\frac{R_{i-1}}{R_i}\omega_{i-1} + \frac{\dot{e}_i}{R_i\cos(\beta)}$, with $e_i = \cos(\beta)[\sin(\omega_{i-1}t - \phi_{i-1})\epsilon_{i-1} - \sin(\omega_i t - \phi_i)\epsilon_i]$, the deviation due to the eccentricity defect of the gear, ϕ_i the initial eccentricity phases and ϵ_i the eccentricity magnitude, $i \in \{2, 4\}$,

- $F_{2ec} = [k_1(t)\delta e R_1\cos(\beta) \;\; k_1(t)\delta e R_2\cos(\beta) \;\; k_2(t)\delta e \;\; R_3\cos(\beta) \;\; k_2(t)\delta e R_4\cos(\beta)]^T$, with δe the initial deviation due to the eccentricity.

In our case, without loss of generality, the eccentricity effect due to the potential energy F_{2ec} is neglected, since the eccentricity fault affects the gear system on the inertia of the system (so, in our model, its impact is already taken into account in the expressions of $\dot{\omega}_i$ and we keep the term due to the kinetic energy F_{1ec} only).

The crack defect F_c is given by $F_c = [R_1\cos(\beta)\Delta k_{1p}(t) \;\; R_2\cos(\beta)\Delta k_{1w}(t) \;\; R_3\cos(\beta)\Delta k_{2p}(t) \;\; R_4\cos(\beta)\Delta k_{2w}(t)]^T$. The term $\Delta k_{jp}(t)$ (respectively, $\Delta k_{jw}(t)$) characterizes the variation of the time-varying gear-mesh stiffness $k_j(t)$ associated to the pinion (respectively to the wheel) of the jth stage of the gearbox system (in our application, $j \in \{1, 2\}$). These quantities are indeed the product between the time-varying gear-mesh variation and the deviation due to the crack. The fault vector F_c will be indicated through the drop of the time-varying stiffness of the gears $k_j(t)$, $j \in \{1, 2\}$. In the healthy functioning case of the gear (without faults), the global time-varying stiffness is a square wave function that normally evolves, for a spur gear, between a maximum value that corresponds to the maximum number of segments in contact (two pairs of teeth) and a minimum value corresponding to the minimum number of segments in contact (one pair of teeth in contact), see Figure 2a, where t_{m1} is the meshing gear period for the first stage of the gearbox system. The descent

in the curves (see Figure 2a) defines the progressive exit of a tooth pair from the meshing zone and the rise corresponds to the gradual entry of a new pair of teeth in contact. In the presence of defects, the disturbances appear on the temporal evolution of the global time-varying stiffness $k_1(t)$ (see Figure 2b, for the first stage) at the moments of the passage of the defective tooth (here, $Z_1 = 18$) in the zone of contact (see, *e.g.,* [10], [43]).

In the faults modeling, we also take into account constant sensor faults $\Delta\theta_1$, $\Delta\theta_2$, $\Delta\theta_3$ and $\Delta\theta_4$ (corresponding, for instance, to offset faults), related to the two gear displacements. The faulty model considering the crack, eccentricity and sensor faults is given by the following system (compare it to (37), the healthy model):

$$\begin{cases} \dot{\theta}_1 = \Omega_1, \\ \dot{\theta}_2 = \Omega_2, \\ \dot{\theta}_3 = \Omega_3, \\ \dot{\theta}_4 = \Omega_4, \\ \dot{\Omega}_1 = \frac{1}{I_1}[-K_{11}\theta_1 - K_{12}\theta_2 - C_{11}\Omega_1 - C_{12}\Omega_2 + C_m \\ \qquad +R_1\cos(\beta)\Delta k_{1p}(t)], \\ \dot{\Omega}_2 = \frac{1}{I_2+I_s}[-K_{21}\theta_1 - K_{22}\theta_2 - K_{23}\theta_3 - C_{21}\Omega_1 \\ \qquad -C_{22}\Omega_2 - C_{23}\Omega_3 + R_2\cos(\beta)\Delta k_{1w}(t) + I_2\dot{\omega}_2], \\ \dot{\Omega}_3 = \frac{1}{I_3+I_s}[-K_{32}\theta_2 - K_{33}\theta_3 - K_{34}\theta_4 - C_{32}\Omega_2 \\ \qquad -C_{33}\Omega_3 - C_{34}\Omega_4 + R_3\cos(\beta)\Delta k_{2p}(t)], \\ \dot{\Omega}_4 = \frac{1}{I_4}[-K_{43}\theta_3 - K_{44}\theta_4 - C_{43}\Omega_3 - C_{44}\Omega_4 + C_r \\ \qquad +R_4\cos(\beta)\Delta k_{2w}(t) + I_4\dot{\omega}_4], \end{cases} \tag{41}$$

with the measurements:

$$\begin{aligned} y_1 &= \theta_1 + \Delta\theta_1, \\ y_2 &= \theta_2 + \Delta\theta_2, \\ y_3 &= \theta_3 + \Delta\theta_3, \\ y_4 &= \theta_4 + \Delta\theta_4. \end{aligned} \tag{42}$$

The appearance of these faults in the gearbox system modify directly the dynamical behavior of the system. It must be noted that the faulty system (41) is a non-autonomous system that depends explicitly on time (*i.e.,* the drift and the vector fields associated to the faults involve explicitly the t-variable through the terms K_{ij}, $1 \leq i, j \leq 4$, $\Delta k_{jp}(t)$ and $\Delta k_{jw}(t)$, for $j \in \{1, 2\}$). In order to transform it into form (6), the state extension explained in Remark 3.4 is applied, that is, we add to system (41) the following equation $\dot{t} = 1$. From now on, when we say system (41), we will actually refer to the extended system associated to (41). Moreover, notice that in system (37), the measurements correspond indeed to states of the system $y_i = \theta_i$, for $1 \leq i \leq 4$. Thus, we do not need to make the change of coordinates explained in the second section since system (41) is already in form (6). We will denote the faulty dynamics of (41), *i.e.,* the right-hand side of (41), by $F(\theta, \Omega)$.

The total number of possible faults is much larger than 4 (the number of the monitoring sensors, see (38)). Therefore, the SRD method can be applied. In the next part, we will apply it in order to detect, identify and locate possible faults.

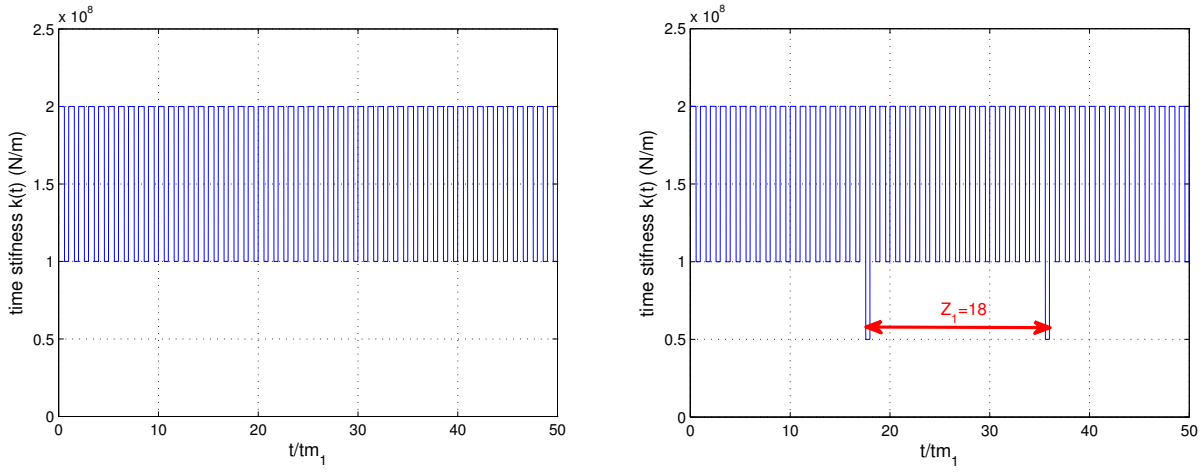

(a) without fault (b) with fault

Figure 2: Time-varying stiffness evolution divided by the meshing gear period t_{m1}

4.3 Application of the sparse recovery method

We define the global fault vector $d(t)$ that contains, not only the faults signatures but as mush information as possible (see Remark 3.1):

$$d(t) = \begin{pmatrix} \Delta\theta_1 \\ \Delta\theta_2 \\ \Delta\theta_3 \\ \Delta\theta_4 \\ R_1\cos(\beta)\Delta k_{1p}(t) \\ R_2\cos(\beta)\Delta k_{1w}(t) \\ R_3\cos(\beta)\Delta k_{2p}(t) \\ R_4\cos(\beta)\Delta k_{2w}(t) \\ I_2\dot{\omega}_2 \\ I_4\dot{\omega}_4 \end{pmatrix} \in \mathbb{R}^{10}. \tag{43}$$

In order to get relation (19) between the measurement vector χ and the fault vector $d(t)$, we first compute the relative degrees of the outputs $y_1 = \theta_1 + \Delta\theta_1$, $y_2 = \theta_2 + \Delta\theta_2$, $y_3 = \theta_3 + \Delta\theta_3$ and $y_4 = \theta_4 + \Delta\theta_4$ as presented in (13) (recall that the sensor faults are supposed piecewise-constant). For instance, consider y_1 (the same calculation has to be done for y_2, y_3 and y_4):

$$\begin{cases} y_1 = \theta_1 + \Delta\theta_1, \\ \dot{y}_1 = \dot{\theta}_1 = \Omega_1, \\ \ddot{y}_1 = \dot{\Omega}_1 = F_5(\theta_1, \theta_2, \Omega_1, \Omega_2), \end{cases} \tag{44}$$

where $F_5 = \frac{1}{I_1}[-K_{11}\theta_1 - K_{12}\theta_2 - C_{11}\Omega_1 - C_{12}\Omega_2 + C_m + R_1\cos(\beta)\Delta k_{1p}(t)]$ describes the faulty dynamics of $\dot{\Omega}_1$, see (41).

In order to extract the sensor faults, we replace the states θ_1 and θ_2 in $F_5(\theta_1, \theta_2, \Omega_1, \Omega_2)$

by their measured values $\theta_1 + \Delta\theta_1$ and $\theta_2 + \Delta\theta_2$ (*i.e.,* with the presence of the sensor faults):

$$\ddot{y}_1 = F_5(\theta_1 + \Delta\theta_1, \theta_2 + \Delta\theta_2, \Omega_1, \Omega_2), \tag{45}$$

$$\begin{aligned} &= \frac{1}{I_1}[-K_{11}(\theta_1 + \Delta\theta_1) - K_{12}(\theta_2 + \Delta\theta_2) - C_{11}\Omega_1 \\ &\quad - C_{12}\Omega_2 + C_m + R_1\cos(\beta)\Delta k_{1p}(t)]. \end{aligned} \tag{46}$$

Applying the same principle for the remaining outputs, we obtain:

$$\ddot{y}_2 = F_6(\theta_1 + \Delta\theta_1, \theta_2 + \Delta\theta_2, \theta_3 + \Delta\theta_3, \Omega_1, \Omega_2, \Omega_3), \tag{47}$$

$$\ddot{y}_3 = F_7(\theta_2 + \Delta\theta_2, \theta_3 + \Delta\theta_3, \theta_4 + \Delta\theta_4, \Omega_2, \Omega_3, \Omega_4), \tag{48}$$

$$\ddot{y}_4 = F_8(\theta_3 + \Delta\theta_3, \theta_4 + \Delta\theta_4, \Omega_3, \Omega_4), \tag{49}$$

where F_6, F_7 and F_8 describe, respectively, the faulty dynamics of Ω_2, Ω_3 and Ω_4, see (41) for their expressions. When developing, (46)-(49) become:

$$\ddot{y}_1 = L_f^2 h_1 - \frac{K_{11}}{I_1}\Delta\theta_1 - \frac{K_{12}}{I_1}\Delta\theta_2 + \frac{R_1\cos(\beta)\Delta k_{1p}(t)}{I_1}, \tag{50}$$

$$\begin{aligned} \ddot{y}_2 = L_f^2 h_2 &- \frac{K_{21}}{I_2 + I_s}\Delta\theta_1 - \frac{K_{22}}{I_2 + I_s}\Delta\theta_2 - \frac{K_{23}}{I_2 + I_s}\Delta\theta_3 \\ &+ \frac{R_2\cos(\beta)\Delta k_{1w}(t)}{I_2 + I_s} + \frac{I_2\dot{\omega}_2}{I_2 + I_s}, \end{aligned} \tag{51}$$

$$\begin{aligned} \ddot{y}_3 = L_f^2 h_3 &- \frac{K_{32}}{I_3 + I_s}\Delta\theta_2 - \frac{K_{33}}{I_3 + I_s}\Delta\theta_3 - \frac{K_{34}}{I_3 + I_s}\Delta\theta_4 \\ &+ \frac{R_3\cos(\beta)\Delta k_{2p}(t)}{I_3 + I_s}, \end{aligned} \tag{52}$$

$$\begin{aligned} \ddot{y}_4 = L_f^2 h_4 &- \frac{K_{43}}{I_4}\Delta\theta_3 - \frac{K_{44}}{I_4}\Delta\theta_4 + \frac{R_4\cos(\beta)\Delta k_{2w}(t)}{I_4} \\ &+ \dot{\omega}_4. \end{aligned} \tag{53}$$

Notice that the above relations are affine with respect to the sensor faults $\Delta\theta_i$ and they are of form (15).

Following (17), we deduce the measurement vector χ containing the available information about the system (recall that χ denotes the difference between the derivatives of the outputs and the healthy operating dynamics of the system):

$$\chi = \begin{pmatrix} \ddot{y}_1 - \frac{1}{I_1}[-K_{11}\theta_1 - K_{12}\theta_2 - C_{11}\Omega_1 - C_{12}\Omega_2 + C_m] \\ \ddot{y}_2 - \frac{1}{I_2+I_s}[-K_{21}\theta_1 - K_{22}\theta_2 - K_{23}\theta_3 - C_{21}\Omega_1 \\ \qquad -C_{22}\Omega_2 - C_{23}\Omega_3] \\ \ddot{y}_3 - \frac{1}{I_3+I_s}[-K_{32}\theta_2 - K_{33}\theta_3 - K_{34}\theta_4 - C_{32}\Omega_2 \\ \qquad -C_{33}\Omega_3 - C_{34}\Omega_4] \\ \ddot{y}_4 - \frac{1}{I_4}[-K_{43}\theta_3 - K_{44}\theta_4 - C_{43}\Omega_3 - C_{44}\Omega_4 + C_r] \end{pmatrix}, \tag{54}$$

where $\ddot{y}_1$, $\ddot{y}_2$, $\ddot{y}_3$ and $\ddot{y}_4$ are estimated using differentiators (see [15] where a sliding mode differentiator is applied to a single stage of gears). It must be noted that differentiators can be implemented since system (41) verifies the observability property explained in Assumption 3.1. Algorithms very similar to those of [15] are used for the two-stage gear (in particular, the differentiators parameters that have to be suitably chosen in order to ensure rapid and accurate convergence between the real and the estimated system states, have the same order of magnitude as those of [15]) and we do not present them here.

From this and definition (43) of $d(t)$, we determine the matrix $\mathbf{\Phi}(x)$ linking χ and $d(t)$ as in (19):

$$\mathbf{\Phi} = \begin{pmatrix} \frac{-K_{11}}{I_1} & \frac{-K_{12}}{I_1} & 0 & 0 & \frac{1}{I_1} & 0 & 0 & 0 & 0 & 0 \\ \frac{-K_{21}}{I_2+I_s} & \frac{-K_{22}}{I_2+I_s} & \frac{-K_{23}}{I_2+I_s} & 0 & 0 & \frac{1}{I_2+I_s} & 0 & 0 & 1 & 0 \\ 0 & \frac{-K_{32}}{I_3+I_s} & \frac{-K_{33}}{I_3+I_s} & \frac{-K_{34}}{I_3+I_s} & 0 & 0 & \frac{1}{I_3+I_s} & 0 & 0 & 0 \\ 0 & 0 & \frac{-K_{43}}{I_4} & \frac{-K_{44}}{I_4} & 0 & 0 & 0 & \frac{1}{I_4} & 0 & \frac{1}{I_4} \end{pmatrix}. \tag{55}$$

An important observation is that in our application, the matrix $\mathbf{\Phi}(x)$ depends explicitly on time through the K-coefficients.

Recall that the SRD method guarantees that at most s faults can be accurately detected and according to Assumption 3.2, the integer s should verify $2s + 1 \leq m$, where m is the number of the monitoring sensors (here, we have $m = 4$). Thus, the SRD method guarantees that at most one fault can be accurately detected for the gearbox model (however, we will see in the next section that, in general, we are able to accurately detect more than one fault). This point can be seen as a limitation of the method but it is justified by the fact that in the industries (and in particular for mechanical systems), the presence of several simultaneous faults is not commun because they generate large disturbances in the system and leads to the extreme case when the machine stops.

One of the most important conditions of the SRD method is that $\mathbf{\Phi}(x)$ has to satisfy the s-order RIP property (here, with $s = 1$), see Definition 3.4. From (55), it can be noticed that some columns are proportional (*i.e.,* the faults corresponding to these columns, here, the sixth and the ninth columns of $\mathbf{\Phi}(x)$, respectively, the eighth and the tenth columns of $\mathbf{\Phi}(x)$, act in the same way on the system). Therefore, we deduce immediately that $\mathbf{\Phi}(x)$, given by (55), does not verify the s-order RIP condition. Moreover, even if we define the global fault vector $d(t)$ with the help of the faults signatures only (that is, in (43), the terms $R_i \cos(\beta)$, for $1 \leq i \leq 4$, I_2 and I_4 are absent), its associate matrix $\mathbf{\Phi}(x)$ would not satisfy the s-order RIP property either. Finally, observe that not all columns of the matrix $\mathbf{\Phi}(x)$ are normalized with respect to the 2-norm. Thus, we have to modify the fault vector $d(t)$, as explained in Remark 3.2, by multiplying the faults associated to the non normalized components of $\mathbf{\Phi}(x)$ by their corresponding norm and regrouping the defects which generate

the collinearity of the columns:

$$d(t) = \begin{pmatrix} n_1\Delta\theta_1 \\ n_2\Delta\theta_2 \\ n_3\Delta\theta_3 \\ n_4\Delta\theta_4 \\ \frac{R_1\cos(\beta)\Delta k_{1p}(t)}{I_1} \\ \frac{R_2\cos(\beta)\Delta k_{1w}(t)}{I_2+I_s} + \frac{I_2\dot{\omega}_2}{I_2+I_s} \\ \frac{R_3\cos(\beta)\Delta k_{2p}(t)}{I_3+I_s} \\ \frac{R_4\cos(\beta)\Delta k_{2w}(t)}{I_4} + \dot{\omega}_4 \end{pmatrix} \in \mathbb{R}^8, \tag{56}$$

with $n_1 = \|\mathbf{\Phi}_1(x)\|_2$, $n_2 = \|\mathbf{\Phi}_2(x)\|_2$, $n_3 = \|\mathbf{\Phi}_3(x)\|_2$ and $n_4 = \|\mathbf{\Phi}_4(x)\|_2$, where $\mathbf{\Phi}_i(x)$ denotes the *ith* column of (55) and n_i is its 2-norm.

In this case, the normalization of the matrix $\mathbf{\Phi}(x)$ is required since it contains different orders of magnitude. By normalizing $\mathbf{\Phi}(x)$, we do not lose the fault vector information and the new matrix (after regrouping the faults and normalization) becomes:

$$\mathbf{\Phi} = \begin{pmatrix} \frac{-K_{11}}{I_1} & \frac{-K_{12}}{I_1 n_2} & 0 & 0 & 1\ 0\ 0\ 0 \\ \frac{-K_{21}}{(I_2+I_s)n_1} & \frac{-K_{22}}{(I_2+I_s)n_2} & \frac{-K_{23}}{(I_2+I_s)n_3} & 0 & 0\ 1\ 0\ 0 \\ 0 & \frac{-K_{32}}{(I_3+I_s)n_2} & \frac{-K_{33}}{(I_3+I_s)n_3} & \frac{-K_{34}}{(I_3+I_s)n_4} & 0\ 0\ 1\ 0 \\ 0 & 0 & \frac{-K_{43}}{I_4 n_3} & \frac{-K_{44}}{I_4 n_4} & 0\ 0\ 0\ 1 \end{pmatrix}. \tag{57}$$

It must be noted that with the new representation, we remain in the over complete matrix case (*i.e.,* the number of monitoring sensors is smaller than the number of faults, $m = 4, q = 8$). The next section presents the simulations results obtained for different activated faults as well as for different cases of s. We will first see that, in accordance with the theoretical results, when only one fault acts on the system, that fault is always correctly diagnosed by the SRD method. Second, we will see that the SRD method works also in many cases when two faults are activated.

5 Simulations and results

In order to evaluate the performances of the SRD method, simulations are carried on Matlab/Simulink. The system parameters are given in Table 3. The designed system was implemented with an *ode*1 *Euler* (we choose this solver because system (30) is not $\mathcal{C}^1$-smooth), and with the exponential coefficient α of (30) being $\alpha = 0.5$ (assuring a convergence in finite-time). Notice that the considered faults have very different order of magnitude and we have to take this into account when choosing the algorithm parameters λ and τ: $\lambda_i = 10^{-2}, \tau_i = 10^4$ for $1 \leq i \leq 4$ (associated to sensor faults) and $\lambda_i = 10^7, \tau_i = 10^{-10}$ for $5 \leq i \leq 8$ (associated to operating faults). This choice of parameters is due to in the system modeling, that is, we consider different types of faults with different orders of magnitude. Notice that if all faults have the same order of magnitude, the same parameters λ and τ can be used for all of them, see [39]).

Simulations results show the good performances of the SRD method to diagnose several mechanical faults in the gearbox system developed in the previous section. Scenario 1 presents

Table 3: Gear parameters

The first stage parameters	Values
Module	2.5 mm
Tooth number of the pinion Z_1	18
Tooth number of the wheel Z_2	26
Face width	20mm
Pressure angle	20 deg
Helix angle β (spur gear)	0 deg
Base radius of the pinion R_1	21 mm
Base radius of the wheel R_2	30 mm
Rotational speed N_1	1674 rpm
Rotational speed N_2	1159 rpm

The second stage parameters	Values
Module	2 mm
Tooth number of the pinion Z_3	20
Tooth number of the wheel Z_4	35
Face width	38mm
Pressure angle	20 deg
Helix angle β (spur gear)	0 deg
Base radius of the pinion R_3	18 mm
Base radius of the wheel R_4	32 mm
Rotational speed N_3	1159 rpm
Rotational speed N_4	662 rpm

the case when only one sensor fault occurs, *i.e.,* $s = 1$, (recall that, according to Assumption 3, we can accurately detect one fault among the eight possible). Scenario 2 explains the case when crack faults occur. Scenario 3 considers two merged faults (crack and eccentricity) that are activated (notice that we are still in the case $s = 1$, since for the modified fault vector, the two original faults are merged into a single one). Scenario 4 illustrates several examples when two different faults occur simultaneously (*i.e.,* $s = 2$). Scenario 5 shows the application of the SRD method when the measurements of the system are affected by a random noise. The non activated faults are set to zero and for all scenarios the corresponding estimates converge to zero. The last scenario (scenario 6) shows the application of SRD method with non-stationary operating conditions.

For each scenario, the figures show all real defects $d_i(t)$, $1 \leq i \leq 8$, and the estimated ones $\hat{d}_i(t)$, $1 \leq i \leq 8$. Presenting all curves on the same figure allows us to highlight the sparsity of the fault vector as well as the fact that (after a short transient time) the estimates of the non-activated faults (those that are identically zero and do not act on the system) converge indeed to zero. Zoomed regions of the estimated faults are carried out in all scenarios in order to show the transient parts. We notice that at the beginning of the algorithm, all estimated faults $\hat{d}_i(t)$, $1 \leq i \leq 8$, varies in time, then the non-activated ones converge to zero. The bold dotted signals represents the activated faults while the bold-solid line signal correspond to their estimation given by the SRD method.

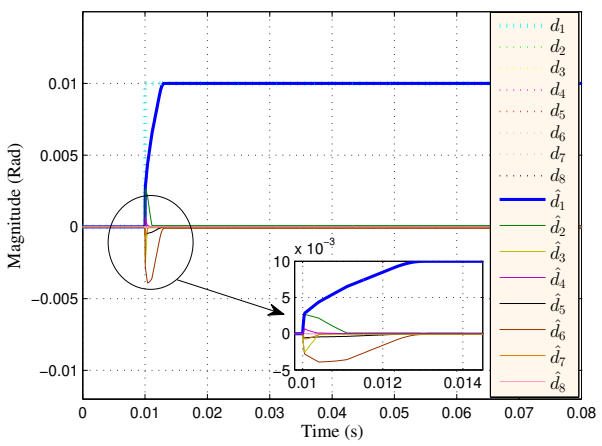

(a) $\Delta\theta_1$ for the first pinion

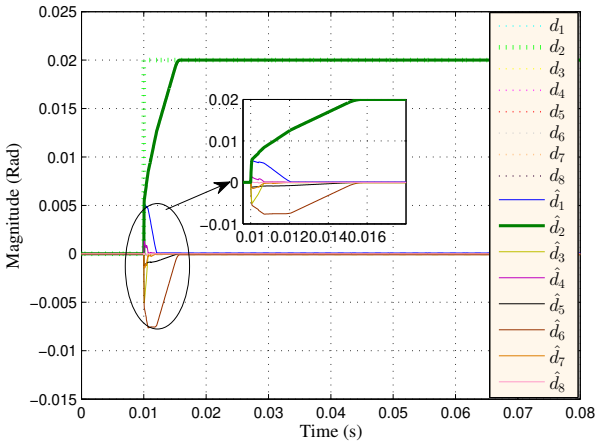

(b) $\Delta\theta_2$ for the first wheel

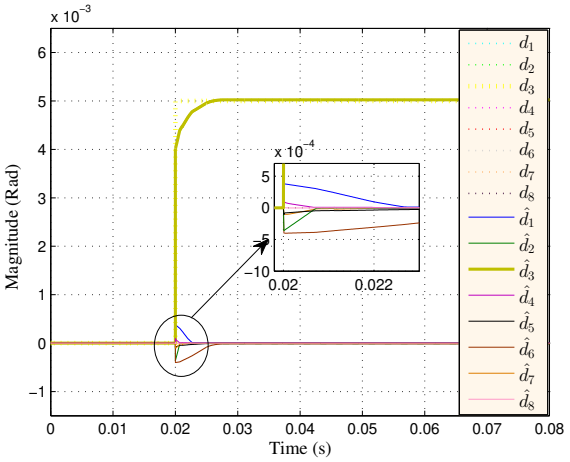

(c) $\Delta\theta_3$ for the second pinion

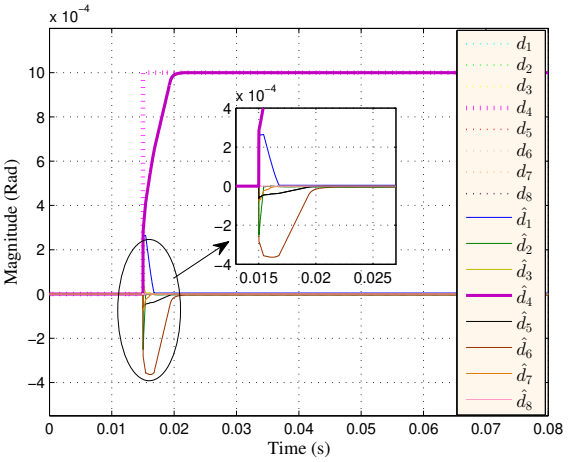

(d) $\Delta\theta_4$ for the second wheel

Figure 3: Scenario 1: Sensor faults

5.1 Scenario 1 ($s = 1$, an activated sensor fault)

This scenario illustrates the case when one fault among the eight possible faults given by (56) is activated. The SRD method is applied four times to extract each of the following faults (for each case of Figure 4a-3d only one of them is activated and the others are set to zero):

$$s_1 = \Delta\theta_1 = \begin{cases} 0, 0 \leq t < 0.01s, \\ 10^{-2}, t \geq 0.01s, \end{cases} \tag{58}$$

$$s_2 = \Delta\theta_2 = \begin{cases} 0, 0 \leq t < 0.01s, \\ 210^{-2}, t \geq 0.01s, \end{cases} \tag{59}$$

that affect the system at $t = 0.01$,

$$s_3 = \Delta\theta_3 = \begin{cases} 0, 0 \leq t < 0.02s, \\ 510^{-3}, t \geq 0.02s, \end{cases} \tag{60}$$

that affects the system at $t = 0.02s$ and

$$s_4 = \Delta\theta_4 = \begin{cases} 0, 0 \leq t < 0.015s, \\ 10^{-3}, t \geq 0.015s, \end{cases} \tag{61}$$

that affects the system at $t = 0.015s$.

Figure 4a-3d show that the activated fault is always accurately recovered in finite-time by the SRD method, while the estimated values of the non activated faults converge to zero. Indeed, from each sub-figure, it is clear that the fault signal $\hat{d}_i$ related to the sensor fault of θ_i, $1 \leq i \leq 4$, converges to its non zero value, while the remaining $\hat{d}_i$ converge to zero. This confirms the good performances of the SRD method to diagnose sensor faults.

5.2 Scenario 2 ($s = 1$, an activated operating fault)

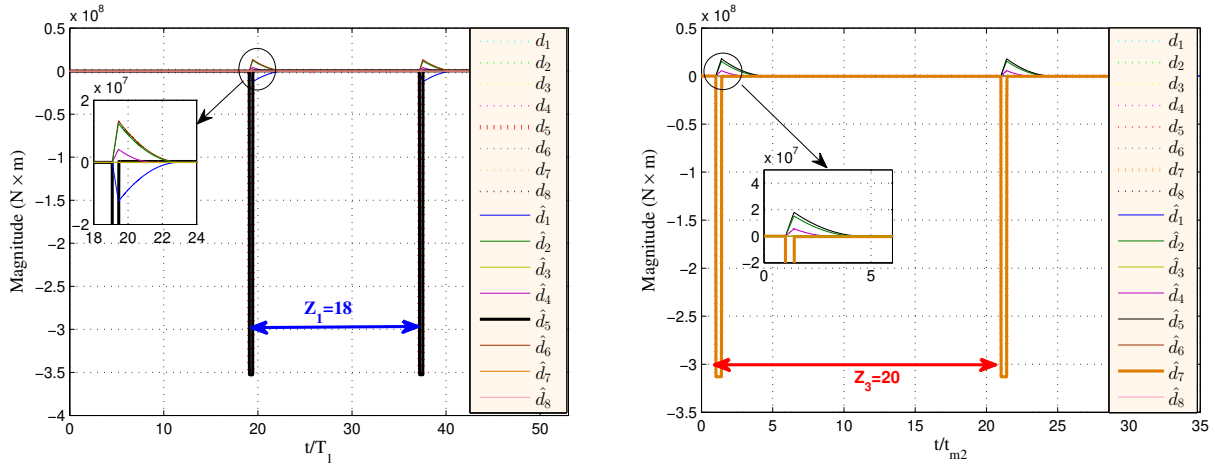

(a) Crack in the first pinion: first stage

(b) Crack fault for the second pinion: second stage

Figure 4: Scenario 2: Crack faults

This scenario presents the case when either the fifth or the seventh fault of $d(t)$ is activated. Both of them are operating faults (corresponding to the presence of the crack in the first or in the second pinion of the gearbox system). It is clear from Figure **??** that the estimated fault $\hat{d}_5$ recovered by the SRD method converges in finite-time to the activated fault and the non activated ones converge to zero. The signal $\hat{d}_5$ is characterized by a time-varying stiffness variation that occurs at each contact of the defective gear and its identification is guaranteed by the signal type (square wave that corresponds to a time-varying stiffness form). Its localization is obtained by the distance between two successive peaks of the time-varying stiffness variation that corresponds to the teeth number of the defective gear. Here, this distance equals to $Z_1 = 18$ in Figure **??** and $Z_3 = 20$ in Figure 4b. The teeth numbers of the defective pinion i, for $i \in \{1, 3\}$ are characteristics of the system which are given in Table 3.

5.3 Scenario 3 ($s = 1$, an activated merged fault corresponding to eccentricity and crack defects)

This scenario corresponds to the case when either the defect d_6 or d_8, regrouping the original crack and the eccentricity faults of the gear, affect the system. We present two cases (for the first one d_6 is activated and $d_8 = 0$, while for the second one $d_6 = 0$ and d_8 is activated). From Figure 5, it is clear that we detect the presence of these faults by the convergence of the estimated defects values to their real values. The distinction between crack and eccentricity

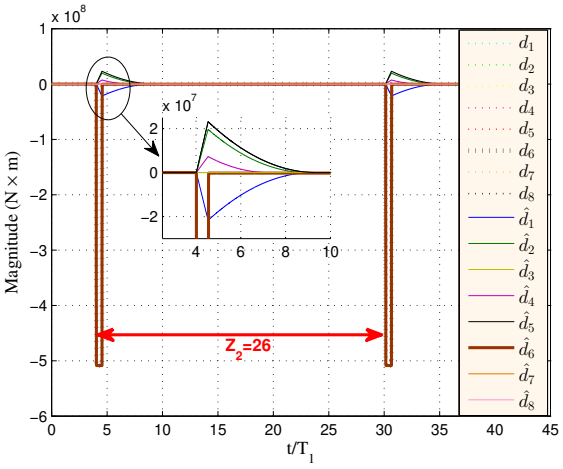

(a) Crack fault for the first wheel: first stage

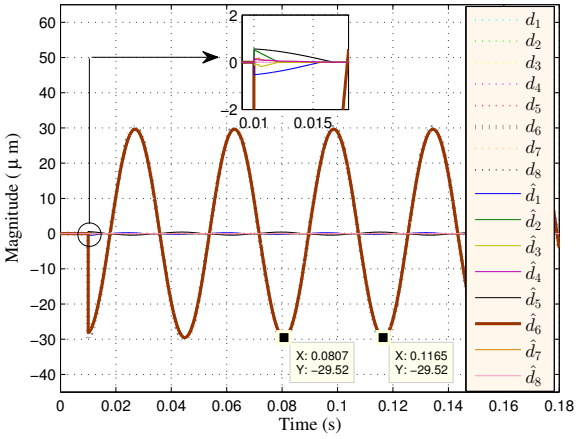

(b) Eccentricity fault for the first stage

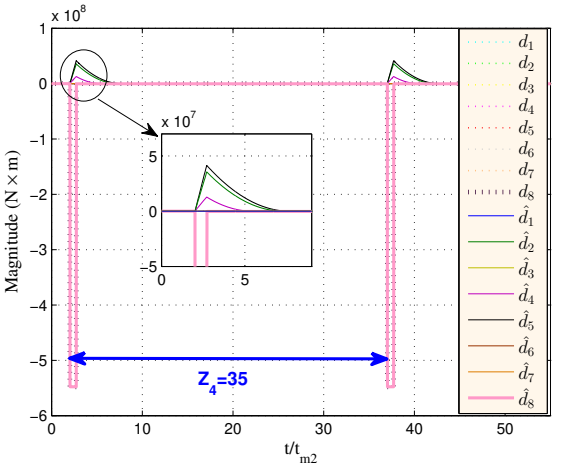

(c) Crack fault in the second wheel: second stage

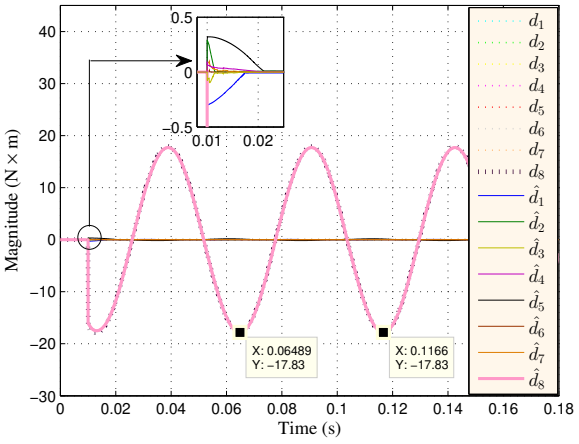

(d) Eccentricity fault for the second stage

Figure 5: Scenario 3: Merged faults

faults is always possible and due to the type of the obtained signals. As explained earlier, the presence of the crack fault is characterized by a square wave signal (here, $Z_2 = 26$ in Figure 5a and $Z_4 = 35$ in Figure 5c, see Table 3) while the appearance of the eccentricity fault is modeled by a sinusoidal form signal (see Figure 5b and 5d). The localization of the eccentricity fault is determined from the rotational speed of the defective gear. For instance, in Figure 5b, the rotational speed of the obtained signal is $w = 2\pi f = \frac{2\pi}{T} = \frac{2\pi}{0.1165-0.0807} = 175.5\ rad/s$ which corresponds to the rotational speed of the first pinion (see Table 3).

In this scenario, a complete localization has been carried out: firstly, we are able to detect the presence of the merged crack and eccentricity faults, secondly, to identify and distinguish them from the obtained signals given by the SRD method, and, finally, to localize them with the help of some characteristics of the mechanical system presented in the obtained signals (*e.g.,* the teeth number, the rotational speed of wheel/pinion).

5.4 Scenario 4 ($s = 2$, two faults occur simultaneously)

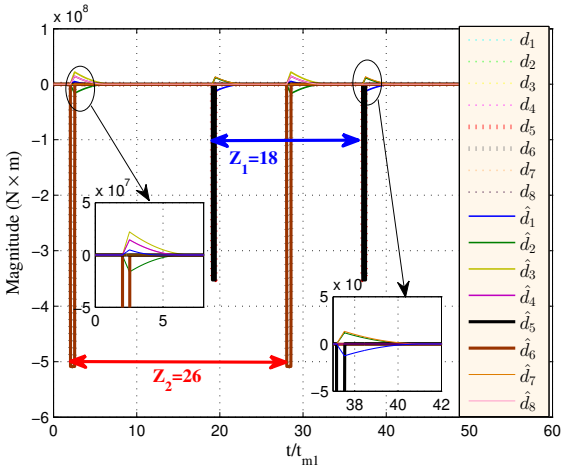

(a) Two activated operating faults

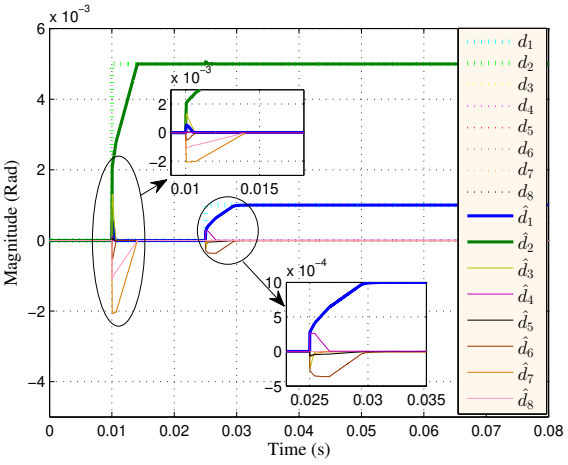

(b) Two activated sensor faults

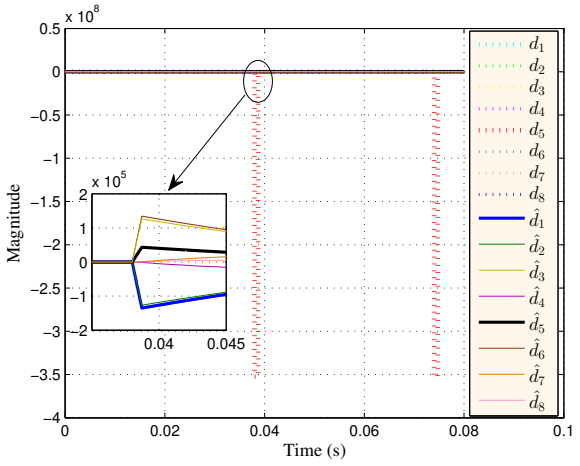

(c) Two activated faults: eccentricity and sensor faults

Figure 6: Scenario 4: Two activated faults $s = 2$

Recall the efficiency of the SRD method is guaranteed for $2s + 1 \leq m$ (in the case of the gearbox application, when only a single fault is activated). A natural question is what happens when at least two faults occur simultaneously. While the previous scenarios present the SRD method results for one active fault, Scenario 4 treats the case when two different operating faults appear simultaneously (see Figure 6)). Figure 6a illustrates the presence, at the same time, of the crack defect in the first pinion and in the first wheel. The SRD method gives a good convergence of the estimated faults to their real values and a complete diagnostic can be carried out. The fault distinction is always possible by the tooth number of the defective gear.

Figure 6b displays the case when two sensor faults related to the displacements θ_1 and θ_2 are activated. We can notice that these activated faults are also accurately recovered in finite-time via the SRD method while the estimated quantities of the non activated faults converge to zero. Thus, we are able to detect the presence of two different faults simultaneously and conclude that the condition $2s + 1 \leq m$ given in Assumption 3.2 is sufficient but not necessary for an accurate reconstruction of the faults using the SRD method.

Figure 6c presents the case when a crack in the first pinion and a sensor fault are activated. It is clear that these faults are not recovered by the SRD method and their diagnostic is not possible. This is due to the fact that the faults have different orders of magnitude. It should be however noted to that our diagnosis method always allows the detection of an anomaly in the system by the non-zero signals given by the SRD method.

Obviously it is possible to diagnose more defects by increasing the number of sensors and therefore, providing more information about the system, and allowing to take into account more possible faults. However, the simultaneous presence of several defects in industrial systems leads to a fast decrease of the equipment life and to a large perturbation or even the stop of the operating system.

5.5 Scenario 5 ($s = 1$, an activated fault in the presence of noises)

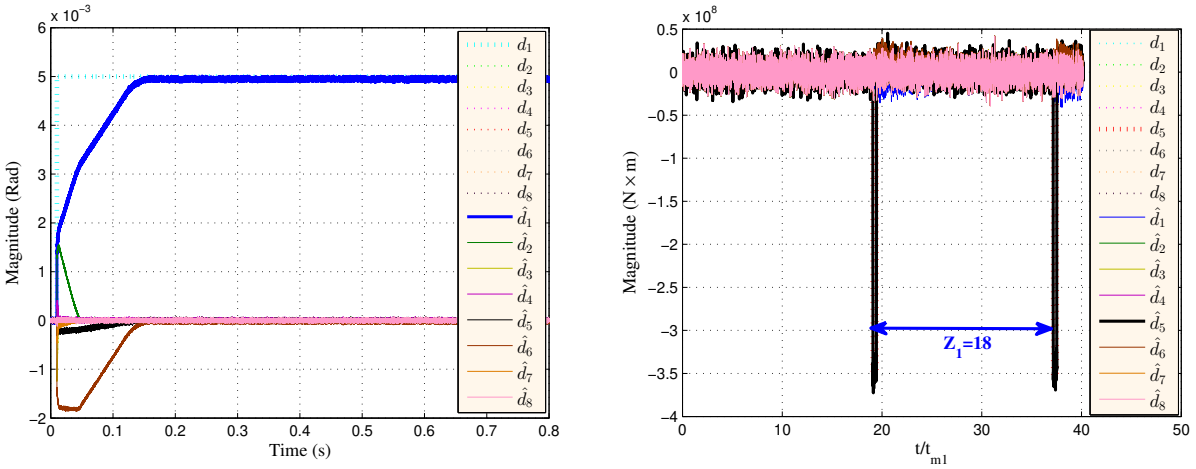

(a) First sensor fault is activated $\Delta\theta_1$

(b) Crack fault of first pinion

Figure 7: Scenario 5: Presence of noise

Usually, the collected sensors signals are polluted by random noises due to the presence of many source of vibration. Scenario 5 considers the case when the measurements are affected by a white random noises. Figure 7a shows the presence of a sensor fault, which is $\Delta\theta_1$, while in Figure 7b a crack fault in the first pinion occurs. For both cases, the estimated faults given by the SRD method converge in finite-time to their real values. The diagnostic of these faults is always possible by analyzing the nature of the obtained signals (as explained in the previous scenarios). Thus, this diagnosis method is still able to identify mechanical and sensor faults by including random measurement noises in the dynamical state-space representation.

5.6 Scenario 6 (non-stationary operating conditions)

The last scenario illustrates the case of non-stationary operating conditions of the gearbox system which is subject to a variable resistant torque. We have considered a load fluctuating in a saw-tooth shape (see Figure 41)).

Figure 9 shows the time evolution of the acceleration of the first stage gear by applying a variable load torque. We notice the presence of peaks that correspond to the peaks of the applied variable load.

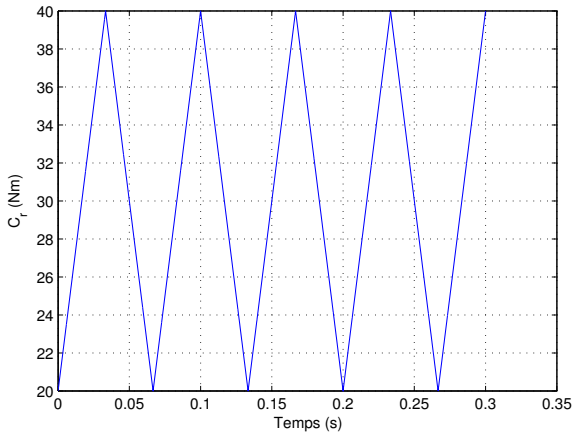

Figure 8: Time evolution of load

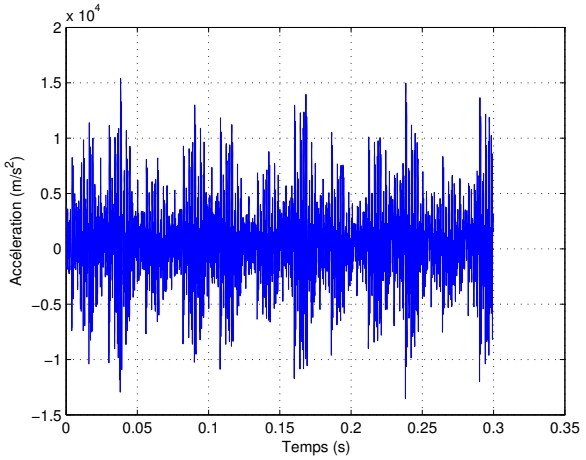

Figure 9: Time evolution of acceleration signal

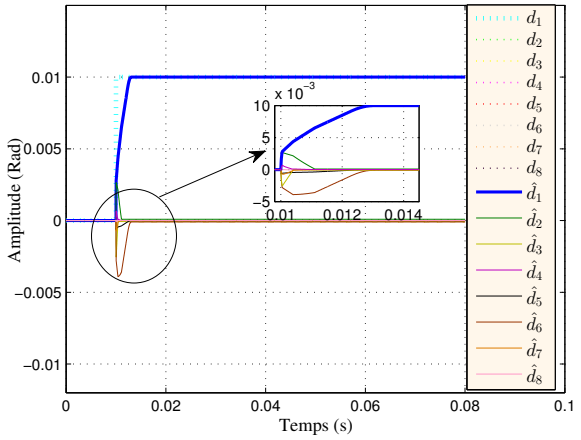

Figure 10: Presence of sensor fault

A sensor fault on the first pinion is activated at $t = 0,01s$. Figure 10 illustrates the good performances of the SRD method in non-stationary conditions.

6 Conclusions

In this paper, a diagnosis method, called sparse recovery diagnosis (SRD), for nonlinear dynamical systems is presented. Then it is applied to the mechanical system of a two-stage gear model. A healthy and faulty modeling of the considered system are presented and implemented via Matlab/Simulink. The SRD is applied in order to diagnose several mechanical faults. Eccentricity, crack and sensor faults are modeled and recovered in finite-time by this diagnosis method. The diagnosis method introduced in this paper is an effective diagnosis method but it is not always able to detect and distinguish all types of defects. For this reason, combining different diagnosis methods is suggested to obtain an optimized and a perfect diagnostic for mechatronic systems. Our future work will be focused on the comparison between other diagnosis techniques and the SRD algorithm as well as on the theoretical generalization of the SRD method for a class of mechanical systems with the presence of different possible faults.

References

[1] Balavoine A, Rozell CJ and Romberg JK (2013) Convergence speed of a dynamical system for sparse recovery. In: *IEEE Transaction Signal Processing* 61(17): 4259–4269.

[2] Barszcz T and Randall RB (2009) Application of spectral kurtosis for detection of a tooth crack in the planetary gear of a wind turbine. In: *Mechanical Systems and Signal Processing* 23(4): 1352–1365.

[3] Besançon G (2007) Nonlinear observers and applications. In: *Springer*, volume 363.

[4] Becker S, Bobin J, and Candes EJ (2011) NESTA: A fast and accurate first-order method for sparse recovery In: *SIAM Journal on Imaging Sciences* 4(1),1-39.

[5] Candes EJ, Romberg JK, and Tao T. (2006) Stable signal recovery from incomplete and inaccurate measurements. Communications on Pure and Applied Mathematics. In: *A Journal Issued by the Courant Institute of Mathematical Sciences* 59(8), 1207-1223.

[6] Candes EJ, Braun N and Wakin MB (2007) Sparse signal and image recovery from compressive samples. In: *2007 4th IEEE International Symposium on Biomedical Imaging: From Nano to Macro*. IEEE, pp. 976–979.

[7] Candes EJ and Wakin MB (2008) An introduction to compressive sampling. In: *IEEE Signal Processing Magazine* 25(2): 21–30.

[8] Chaillet A and Loría A (2008) Uniform semiglobal practical asymptotic stability for non-autonomous cascaded systems and applications. In: *Automatica* 44(2): 337–347.

[9] Chen Y, Shi L, Feng Q, Yang J, Shu H, Luo L, Coatrieux J and Chen W (2014) Artifact suppressed dictionary learning for low-dose ct image processing. In: *IEEE Transactions on Medical Imaging* 33(12): 2271–2292.

[10] Chen Z and Shao Y(2011) Dynamic simulation of spur gear with tooth root crack propagating along tooth width and crack depth. In: *Engineering failure analysis* 18(8), 2149-2164.

[11] Chen X, Du Z, Li J, Li, X and Zhang H (2014) Compressed sensing based on dictionary learning for extracting impulse components. In: *Signal Processing* 96: 94-109.

[12] Combastel C, Lesecq S, Petropol S and Gentil S (2002) Model-based and wavelet approaches to induction motor on-line fault detection In: *Control Engineering Practice* 10 (5), 493-509.

[13] Dai X and Gao Z (2013) From model, signal to knowledge: a data-driven perspective of fault detection and diagnosis. In: *IEEE Transactions on Industrial Informatics* 9(4): 2226–2238.

[14] Derbel S, Feki N, Barbot JP, Nicolau F, Abbes MS and Haddar M (2018) Electromechanical system control based on observers. In: *International Conference on Acoustics and Vibration*. Springer, pp. 101–110.

[15] Derbel S, Feki N, Nicolau F, Barbot JP, Abbes MS and Haddar M (2019) Application of homogeneous observers with variable exponent to a mechatronic system. In: *Proceedings of the Institution of Mechanical Engineers, Part C: Journal of Mechanical Engineering Science* 233(18): 6491–6502.

[16] Derbel S Contribution à la détection des défauts pour la maintenance prédictive des systèmes mécatroniques en utilisant des méthodes basées sur des observateurs: Application à la transmission par engrenages PHD thesis, Cergy Pontoise ENSEA, June 2020

[17] Dong H, Wang Z, Ding SX, and Gao H (2014) A survey on distributed filtering and fault detection for sensor networks. In: *Mathematical Problems in Engineering* 2014: 7.

[18] Dong W, Fu F, Shi G, Cao X, Wu J, Li G and Li X (2016) Hyperspectral image super-resolution via non-negative structured sparse representation. In: *IEEE Transactions on Image Processing* 25(5): 2337–2352.

[19] Du Z, Chen X, Zhang H and Yang B (2017) Compressed-Sensing-Based Periodic Impulsive Feature Detection for Wind Turbine Systems In: *IEEE Transactions on Industrial Informatics* 13(6): 2933-2945.

[20] Fakhfakh T, Walha L, Louati J and Haddar M (2006) Effect of manufacturing and assembly defects on two-stage gear systems vibration. In: *The International Journal of Advanced Manufacturing Technology* 29(9-10): 1008–1018.

[21] Edwards C and Spurgeon S (1998) *Sliding mode control: theory and applications*. In: Crc Press.

[22] Frank PM (1990) Fault diagnosis in dynamic systems using analytical and knowledge-based redundancy: A survey and some new results. In: *Automatica* 26(3): 459 – 474.

[23] Fırat U and Akgül T (2017) Compressive sensing for detecting ships with second-order cyclostationary signatures. In: *IEEE Journal of Oceanic Engineering* 43(4), 1086-1098.

[24] Gao Z, Cecati C and Ding SX (2015) A survey of fault diagnosis and fault-tolerant techniques-part i: Fault diagnosis with model-based and signal-based approaches. In: *IEEE Transactions on Industrial Electronics* 62(6): 3757–3767.

[25] García EA and Frank P (1997) Deterministic nonlinear observer-based approaches to fault diagnosis: A survey. In: *Control Engineering Practice* 5(5): 663 – 670.

[26] Hermann R and Krener A (1977) Nonlinear controllability and observability In: *IEEE Transactions on Automatic Control* 22(5), 728-740.

[27] Hwang I, Kim S, Kim Y and Seah CE (2010) A survey of fault detection, isolation, and reconfiguration methods. In: *IEEE Transactions on Control Systems Technology* 18(3): 636–653.

[28] Isermann R (2005) Model-based fault-detection and diagnosis – status and applications. In: *Annual Reviews in Control* 29(1): 71–85.

[29] Isermann R and Balle P (1997) Trends in the application of model-based fault detection and diagnosis of technical processes. In: *Control Engineering Practice* 5(5), 709-719.

[30] Kimmich F, Schwarte A and Isermann R (2005) Fault detection for modern diesel engines using signal-and process model-based methods. In: *Control engineering practice* 13(2): 189–203.

[31] Lei Y, Lin J, He Z and Zuo MJ (2013) A review on empirical mode decomposition in fault diagnosis of rotating machinery. In: *Mechanical Systems and Signal Processing* 35(1): 108 – 126.

[32] Lin H, Tang, J and Mechefske C (2019) Impulse detection using a shift-invariant dictionary and multiple compressions. In *Journal of Sound and Vibration* 449, 1-17.

[33] Martinez-Guerra R, Mata-Machuca JL, and Rincón-Pasaye, JJ (2013) Fault diagnosis viewed as a left invertibility problem. In: *International Society of Automation Transactions*, 52(5), 652-661.

[34] Nateghi S, Shtessel Y, Barbot JP, Zheng G and Yu L (2018) Cyber-attack reconstruction via sliding mode differentiation and sparse recovery algorithm: Electrical power networks application. In: *2018 15th International Workshop on Variable Structure Systems*. IEEE, pp. 285–290.

[35] Nijmeijer H (1986) Right-invertibility for a class of nonlinear control systems: A geometric approach. In: *Systems and Control Letters*, 7(2), 125-132.

[36] Respondek. W (1990). Right and left invertibility of nonlinear control systems. In *Nonlinear Controllability and Optimal Control*, Routledge New York,(133-176). Routledge.

[37] Takahara Y, Nakano B, and Aaht T. (1984) Structure of left invertibility problem of linear systems. In: *International Journal of Systems Science*, 15(7), 777-795.

[38] Tang G, Yang Q, Wang HQ, Luo, GG and Ma JW (2015) Sparse classification of rotating machinery faults based on compressive sensing strategy. In: *Mechatronics* 31, 60-67.

[39] Torki W, Derbel S, Barbot JP, Sbita L (2019) A novel FDI sparse recovery method: Application on PMSG wind turbine. In: *submitted to Transactions of the Institute of Measurement and Control journal, January, 2020.*

[40] Vo Tan P, Millerioux G and Daafouz J (2010) Left invertibility, flatness and identifiability of switched linear dynamical systems: a framework for cryptographic applications, In: *International Journal of Control*, 83:1, 145-153.

[41] Yang J, Wright J, Huang TS and Ma Y (2010) Image super-resolution via sparse representation. In: *IEEE Transactions on Image Processing* 19(11): 2861–2873.

[42] Yu L, Zheng G and Barbot JP (2017) Dynamical sparse recovery with finite-time convergence. In: *IEEE Transactions on Signal Processing* 65(23): 6146–6157.

[43] Yu, W, Shao Y and Mechefske C (2015) The effects of spur gear tooth spatial crack propagation on gear mesh stiffness. In: *Engineering Failure Analysis* 54, 103-119.

[44] Zheng J, Cheng J, Yang Y and Luo S (2013) A rolling bearing fault diagnosis method based on multi-scale fuzzy entropy and variable predictive model-based class discrimination. In: *Mechanism and Machine Theory* 78, 187 - 200.